Machine Learning for Optimised and Clean Li-ion Battery Manufacturing: Revealing the Dependency between Electrode and Cell Characteristics

Mona Faraji Niri, Kailong Liu, Geanina Apachitei, Luis Roman Ramirez, Michael Lain, Dhammika Widanage, James Marco

Warwick Manufacturing Group, University of Warwick, CV4 7AL Coventry, United Kingdom
The Faraday Institution, Quad One, Harwell Science and Innovation Campus, Didcot, UK (mona.faraji-niri@warwick.ac.uk)

ABSTRACT

The large number of parameters involved in each step of Li-ion electrode manufacturing process as well as the complex electrochemical interactions in those affect the properties of the final product. Optimization of the manufacturing process, although very challenging, is critical for reducing the production time, cost, and carbon footprint. Data-driven models offer a solution for manufacturing optimization problems and underpin future aspirations for manufacturing volumes. This study combines machine-learning approaches with the experimental data to build data-driven models for predicting final battery performance. The models capture the interdependencies between the key parameters of electrode manufacturing, its structural features, and the electrical performance characteristics of the associated Li-ion cells. The methodology here is based on a set of designed experiments conducted in a controlled environment, altering electrode coating control parameters of comma bar gap, line speed and coating ratio, obtaining the electrode structural properties of active material mass loading, thickness, and porosity, extracting the manufactured half-cell characteristics at various cycling conditions, and finally building models for interconnectivity studies and predictions. Investigating and quantifying performance predictability through a systems' view of the manufacturing process is the main novelty of this paper. Comparisons between different machine-learning models, analysis of models' performance with a limited number of inputs, analysis of robustness to measurement noise and data-size are other contributions of this study. The results suggest that, given manufacturing parameters, the coated electrode properties and cell characteristics can be predicted with about 5% and 3% errors respectively. The presented concepts are believed to link the manufacturing at lab-scale to the pilot-line scale and support smart, optimized, and clean production of electrodes for high-quality Li-ion batteries.

KEYWORDS: Li-ion Battery Electrodes, Cathode Manufacturing, Machine Learning, Modelling, Prediction, Optimised Production

1. INTRODUCTION

Lithium-ion battery (LiB) is a popular energy source and plays an important role in applications such as electrified transportation systems and smart grids due to its superiorities in terms of low self-discharge and high energy density. However, A major limitation for LiB's wider applications is its manufacturing technology. According to the literature the production cost of batteries is expected to be reduced from about 400 €/kWh in 2013 to circa 75 €/kWh in 2022 (Turetskyy, et al, 2021). Although the manufacturing cost is declining, it is still highly affected by the waste, scrape rates and process deflections. The amount of material and component waste during manufacturing can be as high as 15% of the total costs (Hanisch, et al, 2015). Beside material waste resulted from the failed batteries at the end of manufacturing processes, the large number of characterisation tests has also a significant impact on the cost as well as carbon emissions in the concepts of clean production (Kwade, et al, 2018). Currently, the LiB manufacturing is responsible for about 50% of Co_2 emissions during production of electrified transportation systems (Turetskyy, et al, 2021). The processes within battery manufacturing chain significantly affect the properties of intermediate products, which would in turn determine the quality of produced batteries (Kwade, et al., 2018; Väyrynen & Salminen, 2012). Consequently, it is vital to well monitor and analyse battery manufacturing chain in the pursuit of producing high-quality and economically affordable batteries, avoiding, or limiting production failures and detecting process deflections at early stages of manufacturing chain (Zwicker, et al, 2020).

Revealing the correlations between the key manufacturing parameters, the intermediate products' characteristics and final battery quality can help achieve an optimised production process by reducing production cost and lowering its environmental impacts.

Battery manufacturing can be generally divided into four processes, including the electrode manufacturing, battery assembly, battery finishing and characterisation. The electrode manufacturing consists of many individual processes such as the mixing, coating, drying, calendaring, and cutting. Each process contains chemical, mechanical, and electrical operations that generate numerous and strongly coupled parameters in the order of tens or hundreds in total. Furthermore, the battery itself is a complex system with interactions between its components such as anode, cathode, electrolyte, and current collectors which eventually determine its energy capacity, internal resistance, and lifetime. The current mainstream strategy to analyse the manufacturing parameters is still based on trial and error, which is significantly time and resource consuming (Thomitzek, et al, 2018). Therefore, a reliable, systematic, and data-oriented strategy to explore and predict the impact variables of manufactured batteries is urgently required but challenging.

Due to the dramatic increase of cloud platforms as well as advanced machine-learning technologies, data-driven strategies are becoming one of the most popular research topics in many industrial domains (Li, et al, 2019; Lipu, et al, 2021).

For battery application, a good deal of studies has focused on developing reasonable machine-learning solutions and data-driven methods to promote battery management activities and improving its performance. In (Niri, et al, 2020a) the battery dynamic states related to its remaining energy are estimated and predicted via Gaussian mixture models for applications with unknown loading conditions. Cells' state of energy index is predicted via multi-layer Markov models in (Faraji, et al, 2019) and verified experimentally for electric vehicle's state of power estimation via wavelet-Markov in (Niri, et al, 2020b). Remaining useful life of batteries is forecasted under variable discharge profiles in (Hong, et al, 2021) by deep-learning methods, while a feature-based approach to build an early-prediction model with a regularized linear structure is proposed by (Severson, et al, 2019). (Liu, et al, 2020a; Tian, et al, 2021) combine physics-based single particle models and artificial intelligence to forecast and optimise battery service and its calendar life. (Lipu, et al, 2020) has reviewed data-driven methods including neural networks, support vector machines and probabilistics algorithms for the battery state of charge estimation. Battery charging controller design and fast charging process optimisation via a Bayesian approach has been addressed by (Attia, et al, 2020), where the experimental data are combined with machine learning techniques to predict the battery life given the data at its early stages of the use. Smart energy management and energy control strategies have been developed in (Wu, et al, 2020; Liu, et al, 2020b), battery thermal modelling and management via Gaussian-Markov models are proposed in (Faraji, et al, 2020a) and a recent review of battery thermal management methods taking the advantage of data-driven approaches in performed by (Lin, et al, 2021). Battery reuse and recycle considerations, addressed by a variety of machine learning models are also reviewed in (Garg, et al, 2020; Liu, et al, 2019).

Evidently, most of these studies have focused primarily on improving produced battery performance but relatively little has been performed on techniques for manufacturing their internal components and providing solutions to benefit the battery manufacturing and production process (Dahodwalla & Herat, 2000; Liu, et al, 2021a) as well as the battery manufacturning flow (He, et al, 2020). The large amount of data generated during production processes when combined with machine-learning techniques would provide an opportunity to establish data-driven models to analyse the battery manufacturing parameters and the final cells' characteristics. According to the recent updates, machine learning is expected to support shortening the development cycle of advanced energy storage systems from decades to only a few years (Mistry, et al, 2021). Following this opportunity, through utilizing a concept of quality gate (Schnell & Reinhart, 2016) has proposed a strategy for diagnosing the failure cases and improving the control performance of battery production. On the basis of an effective framework called cross industry standard process, neural network models are designed in (Schnell, et al, 2019) for the forecast and analysis of the dependencies between the parameters of battery manufacturing processes. The decision tree-based strategies are derived in (Turetskyy, et al, 2020) to quantify the importance weight of manufacturing parameters and forecast related battery maximal capacities. (Cunha, et al, 2020) has utilized machinelearning methods for the electrode property classification and then analysed electrode manufacturing parameters through 2D graphs from experimental data. In (Liu, et al, 2021a; Liu, et al, 2021b) the importance as well as correlations among four parameters from mixing and coating stages are quantified through an interpretable machine-learning framework.

The research also highlights the effect of the key parameters on the mass loading and porosity of cell electrodes.

Recent reviews conclude that although a number of existing works have adopted the data-driven strategies to benefit battery manufacturing, several limitations are not yet addressed. Most of the mentioned studies are aimed at covering the issues related to intermediate products, especially electrodes only. They offer data-driven concepts, standardize the procedures to capture relevant data from production lines, technical building services and cell diagnostics (Turetskyy, et al, 2020), determine the important process steps, identify crucial features (Filz, et al., 2020), and distinguish variables that show the effect of manufacturing control parameters on the quality of the intermediate product (Thiede, et al, 2019; Faraji, et al, 2020b). In particular, (Cunha, et al , 2020) has focused on the effect of mixing and coating control parameters on the characteristics such as mass loading and porosity of the coated electrodes. (Liu, et al, 2021b; Liu, et al, 2021a) have utilised the manufacturing parameters and data recorded by (Cunha, et al , 2020) during electrode manufacturing to build interpretable artificial intelligence models, and (Duquesnoy, et al, 2021) has predicted the homogeneity of electrode structure given the parameters of active material, liquid to solid ratio and coating gap. In (Duquesnoy, et al, 2020) a combination of experimental results, *in silico* generation of electrode mesostructures and machine learning algorithm of Sure independent Screening and Sparsifying Operator are used to link the uncalendared and calendared electrode structure properties. (Chen, et al., 2021) have taken the advantage of various machine-learning models to optimise the fabrication of thin solid state electrolyte films for energy storge application and studied the effect of polymer content, liquid to solid ratio and co-solvent on the film conductivity. Statistical methods of covariance analysis and principal component analysis are utilised in (Primo, et al, 2021) to link the calendaring parameters of cathode manufacturing, (i.e., the applied pressure, roll temperature, and line speed) to the electrode conductivity. Neither of the studies are correlating the key parameters to the final assembled cell's electrochemical performance.

On the other hand, a number of studies such as (Turetskyy, et al, 2021) offer prediction of final product properties, such as battery maximum capacity, via a cyber-physical framework. Data-driven methods are addressed in (Kornas, et al, 2019) to reveal cause-effect relationships between electrolyte mass and final characteristic of maximum capacity. However, the mentioned studies only cover a limited number of key parameters from intermediate to final steps and no correlation to the initial manufacturing parameters has been studied.

Knowing that the quality of the final cell is determined by multiple factors, a lack of a comprehensive study covering the key parameters, intermediate and final product characteristics is obvious. Therefore, this paper investigates how machine-learning algorithms can support the quality prediction of not only the intermediate product's features, but also the performance of the final product in terms of the interested indices.

Here, a design of the experimental methods and modelling process is proposed to predict battery manufacturing quality – a process that traditionally has been based on a qualitative understanding and trial-and-error experience. Furthermore, a set of inputs and outputs, including comma bar gap, coating line speed, coating ratio, coating thickness, porosity, mass loading and cell energy capacity at various C-rates of C/20, C/2, 1C and 2C are considered which have not been discussed in a holistic manner within the previous literature so far and this is the main part of research distinguishing it from the previous ones.

This study follows the four main objectives:

- Provide a comprehensive design of experiment methodology for studying the correlation between electrode manufacturing parameters and product quality.
- Suggest a systematic process for data preparation, data processing, modelling, and property prediction of battery manufacturing processes.
- Determine the most important intermediate and final product parameters that impact battery quality and process efficiency
- Quantify the predictability of structural and electrochemical properties of electrodes and Li-ion cells.

The objects are achieved by offering the ranges, limits, and brake points of control parameters in a real manufacturing line, the full table of designed experiments, the data processing steps, and finally correlation analysis of manufacturing parameters with intermediate product's features. The analysis is then followed by building models and investigating their performance for predicting characteristics of the intermediate and final products.

The main model of this study is based on support vector machine (SVM) and is compared with the widely known prediction algorithms of linear regression (LR), decision tree (DT), feedforward artificial neural network (NN) and gradient boosted trees (GBT). These comparisons quantify the predictability of various parameters via both common and advanced modelling techniques. Further analysis is performed in four main aspects to facilitate the extension of the proposed models from lab scale to the volume manufacturing scale: 1) data size that is necessary for an accurate training and prediction, this analysis suggests an approximate number of the experiments required to build representative models. 2) the sensitivity of models to measurement noise, this analysis is aimed at quantifying the effect of measurement equipment errors and calibrations in real manufacturing processes, 3) predictability analysis considering a limited number of input variables, this part focuses on feature selection and helps to eliminate the cost of experiments for measuring the variables that do not have a significant impact on the prediction accuracy. 4) generalisability and interpolation capability of models to quantify the predictability of electrochemical characteristics via models when the relevant data is not utilised in the training process, this analysis is critical in reducing the number of cycling and characterisation tests at various conditions.

The approach used for design of experiments to gather the data with minimum effort, the methodology of data collection and preparation, performance, and property prediction as well as the comprehensive analysis and discussions mentioned in above are considered as the other novelties of this study compared to the previous research.

It is also worth mentioning that this study is focused on the positive electrode (cathode), is based on calendared coatings, and discusses half-cell performance for simplicity. Without loss of generality, the offered approaches and driven results are a stepping-stone to the complete solution for the performance prediction of full cell Li-ion battery.

The structure of this paper is as follows, in Section 2, the experimental study details are presented. This section contains the details of the electrode manufacturing process, cell manufacturing steps and how the key indices are quantified. Section 3 describes the data preparation and modelling methodology, the predictive models, and comparisons. Section 4 provides results, discussions, and validations under various assumptions. Finally, section 5 gives concluding remarks and challenges to be addressed in future works.

2. EXPERIMENTAL MANUFACTURING STUDY

The pilot-line scale battery manufacturing process is summarized in Figure 1. This study is focused on cathode coating process and the impact of its control parameters on the quality of the electrodes as well as the performance of the manufactured half-cells. For minimizing the effect of the control parameters of other steps, they have been kept constant in between the runs.

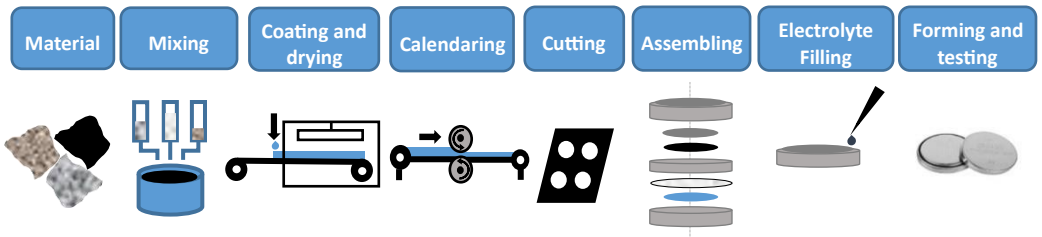

Figure 1 Pilot-line scale battery production chain

Figure 2 (a) Laboratory scale electrode manufacturing line, (b) coating machine

For electrode manufacture a self-metered coating the comma bar technology, Figure 2, has been used which is the gap between the technique, where the coating thickness is determined via adjusting line (i.e., web/line comma bar and the substrates as well as the speed of the coating and after a certain speed). During the experiments, the control parameters were set indicators (KPIs) length of coated electrode was completed, the key performance experiment in were obtained and then settings were altered for the next machine.

2.1 Electrode manufacture

The cathode formulation was 96% active material of nickel, manganese cobalt oxide (NMC 622), 2% conductive additive of carbon black (C65), and 2% of Polyvinylidene fluoride binder. First the dry components were mixed, then the solvent of choice, N-methyl pyrrolidinone was added to create a mixture of appropriate consistency with 77% solid content at the kneading stage. Then, the mixture (slurry) was diluted with further addition of solvent to a final solid content of 67%, Figure 3 (a). Quality checks of the intermediate products were performed via a Hegman gauge, Figure 3 (b) to ensure the fineness of grind and absence of large agglomerates.

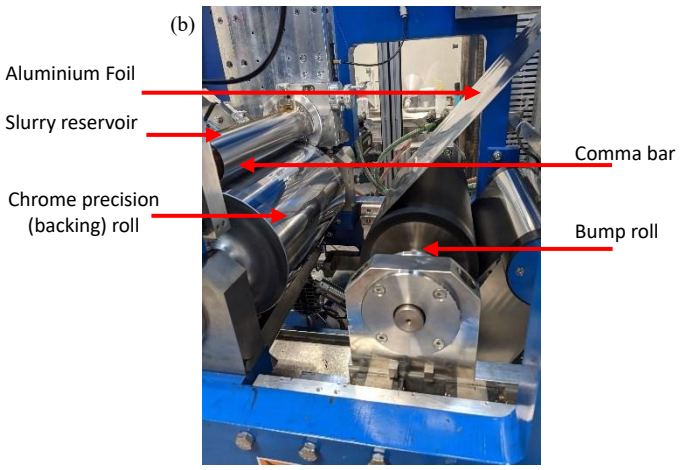

In the next step, the slurry was used to coat a 15 um Aluminium foil to get the cathode electrode. The roll-to-roll coating process was accomplished via a pilot-scale coating machine, Dürr Megtec, with comma bar technology and 3-zone thermal dryer with an effective drying length of about 3.5 meters, Figure 2 (a). During the coating process, the backing roll and the comma bar created a reservoir for the slurry. The coating moved from the reservoir onto the backing roll and then transferred on the current collector which was supported by the bump roll. The foil was guided and supported by both rolls through the ovens, moving with a controlled web/line speed (*m*/*min*).

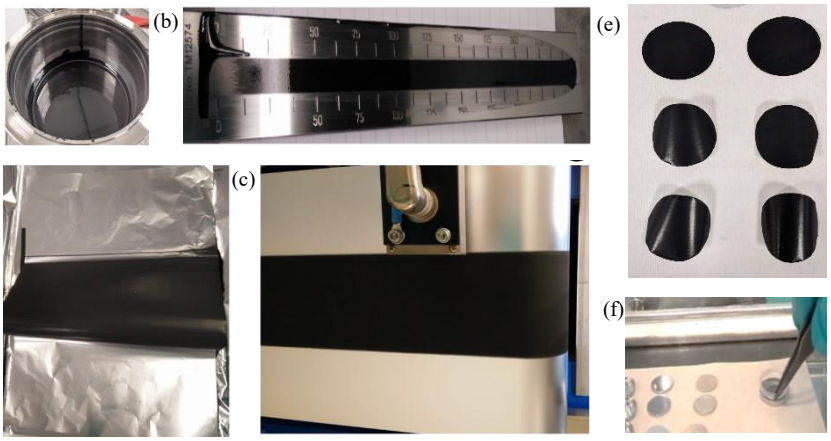

Figure 3 Intermediary products from different manufacturing stages: a) slurry, b) slurry test on Hegman gauge, c) electrode after coating and drying, d) section of calendared electrode, e) die-cut electrodes at different stages during calendaring, f) assembly

The quantity of slurry released onto the backing roll was controlled by the comma bar gap (*um)*, the gap between comma bar and backing roll. The rate of transfer from the chrome roll to the foil, called coating ratio (*%*), referred to the ratio of the bump roll speed (for which the reference was the web speed) to the backing roll speed and was also used to control the mass loading of the coating, Figure 2 (b). After coating, the electrodes were dried overnight for 12 hours in a Binder^{TM} vacuum furnace. During drying, the solvent was evaporated under controlled temperature of 120 °*C*, the conditions were kept unchanged for all experiments to minimize the effect of the drying control parameters on the coating and cell characteristics. Then, the coating was calendared to a target porosity of 30%. Intermediate products including electrodes after coating, and calendaring are given in Figure 3 (c) and (d) respectively.

2.2 Quantifying electrode KPIs

On total three properties of mass loading (g/m^2), thickness (*um*), and porosity (%) were measured/calculated for each manufactured electrode. For mass loading of the electrode, which is the weight of the active material on the electrode per unit area, the MeSys GmbH machine was used with ultrasound sensors located at ~0.3*mm* intervals, one output value per 6 seconds and an accuracy of +/- 2 g/m^2. Thickness of the electrodes was measured by a digital micrometre, Mitutoyo,

with the accuracy of about 1 *um*. Measurements were obtained from 10 different locations on electrode surface and then averaged. After measuring the electrode mass loading and thickness, electrode porosity (%) was calculated by (1).

$$Porosity = \frac{1 - V^{nom}}{} = \frac{A\ Gsm*}{V_{act}\ \rho_{avg} * Th} \quad (1)$$

While V_{nom} (cm^3) is the nominal volume of cathode coating. V_{act} denotes the actual volume of the electrode as (2), and it will simplify the porosity to (3).

$$V_{nom} = \frac{A\ Gsm*}{\rho_{avg}},\ V_{act} = A\ Th* \quad (2)$$

Here, *Gsm* is the coating mass loading (g/m^2), *Th* denotes the coating thickness (*um*) and ρ_{avg} is the average density of the electrode (g/cm^3) and *A* the coating area in (m^2).

$$Porosity = \frac{A\ Gsm*}{\rho_{avg} * Th} \quad (3)$$

2.3 Coin-cell manufacture

After producing the electrodes and measuring their key parameters, each piece of electrode was used to manufacture at least three cells. For this purpose, the electrode discs with a diameter of 14.8 mm^2 were obtained by die-cutting, Figure 3 (e). They were left for drying once again before assembly for another 12 hours in 120°C. The cut electrodes, (i.e., cell electrodes) were measured/calculated once again for thickness (*um*), mass loading (g/m^2), and porosity (%) by micrometre, high precision scale and the equations of (1) to (3). Finally, half-cells (2032 coin cells), with lithium metal as the counter electrode, were made by stacking electrodes, separator and Li-ion discs, adding electrolyte and crimping the cell case in a nitrogen filled box, Figure 3 (f). In total 115 half coin cells were left after excluding failed ones. It is worth pointing that here half-cells were preferred over full cells to keep focus on cathode manufacturing.

2.4 Quantifying coin-cell KPIs

After assembly, the half-cells went through a formation cycle at C/20, 5 conditioning cycles at C/5, then characterisation cycling at different C-rates using Maccor™ battery testing equipment connected to a Binder™ thermal chamber at 25°C. The capacity of half-cells (*mAh*) was obtained by constant current, constant voltage discharge at low (C/20, C/5), medium (C/2 and 1C) as well as high (2C) C-rate for a comprehensive analysis. All samples were gone through a C/5 charging process at the similar cycling conditions after each characterisation test.

2.5 Design of experiments

As running the experiments are quite time and resource consuming, here a design of experiments (DoE) approach was used to obtain as much information as possible from the minimum of experiments. DoE is to reduce the total amount of experiments required for the identification of the main influencing factors of the electrode manufacturing process and study their effect on electrode mass loading, thickness, and porosity as well as performance.

The DoE consisted of two parts, in the first part, a screening design was employed to identify the main influencing factors of the coating process and determine their effect on the physical characteristics of the electrode as well as electrochemical

performance. In the second part, a response surface methodology (RSM) was used to gather further information on the identified main factors (Oehlert, 2010).

The screening design consisted of a fractional factorial saturated design (Steinberg, 1996) where five main factors were considered into account, involving two extreme settings for each. These factors and their settings were chosen based on recommendations from the literature (Cunha, et al , 2020; Mishra, et al., 2018) and feedback from expert users.

The initial factors included, comma bar gap (80 and 140 *um*), coating ratio (110 and 150 %), web speed (0.5 and 1.5 *m/min*), drying air speed (5 and 15 *m/s*) and drying temperature (85 and 110 °*C*). The drying process was designed to take place in a dryer with three zones and independent temperature settings. Nevertheless, to keep the number of factors

limited, only the upper section temperature was considered as a key factor here. Furthermore, for simplicity, the air speed for all three sections were kept the same. The screening DoE matrix was comprised of 12 experimental runs at different conditions as in Table 1.

Table 1 Experiments for the screening DoE

Experiment number	1	2	3	4	5	6	7	8	9	10	11	12
Comma bar gap (*um*)	140	80	80	140	80	80	140	140	140	140	80	80
Web speed (*m/min*)	0.5	0.5	1.5	0.5	1.5	1.5	1.5	1.5	1.5	0.5	0.5	0.5
Temperature (°*C*)	85	85	110	110	85	110	110	85	85	110	85	110
Air speed (*m/s*)	5.0	15	5.0	5.0	5.0	15	5.0	15	15	15	5.0	15
Coating ratio (*%*)	150	150	150	110	110	110	150	110	150	110	110	150

Since the analysis of the output variables revealed a strong correlation only for comma bar gap, web speed and coating ratio, a second DoE of RSM type was employed focused on these three factors. The RSM consisted of a Box-Wilson composite design (CCD) involving five levels for each of the factors (Myers, et al , 2016). Because the ranges used in the screening DoE were identified as practical limits for the factor settings, an inscribed CCD (CCID) was finally used in which the factor levels are inside the region given by the extreme settings (i.e., comma bar gap: 80, 92, 110, 128 and 140 *μm*; web speed: 0.5, 0.7, 1.0, 1.3 and 1.5 *m/min*, and coating ratio: 110, 118, 130, 142 and 150 *%*). A graphical representation of the CCID is shown in Figure 4.

It is worth mentioning that this DoE consists of 6 centre runs to provide stability of the variance and is consisted of 20 runs reported in Table 2. The combination of both screening and CCID resulted 32 experiments that were all combined for modelling purposes.

Table 2 Experiments for the CCID DoE

Experiment number	1	2	3	5	6	7	8	9	10	12	13	14	17	18	19	20
													128	110	128	110
Comma bar gap (*um*)	128	110	80	110	110	128	92	92	110	92	110	140	110	92		
Web speed (*m/min*)	0.7	1.0	1.0	1.5	1.0	0.7	1.3	0.7	1.0	0.7	1.0	1.0	1.0	1.3	1.0	1.0	1.3	0.5	1.3	1.0
Coating ratio (*%*)	142	130	130	130	110	118	142	142	130	118	130	130	130	118	150	130	118	130	142	130

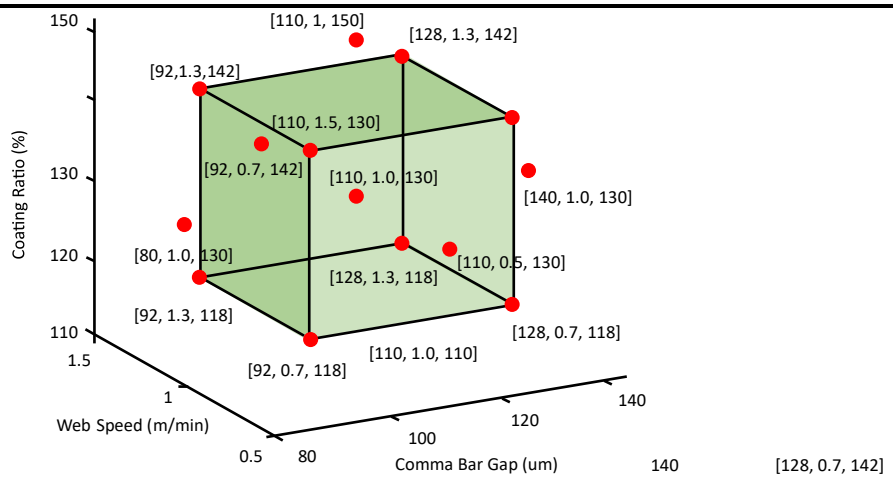

Figure 4 Graphical representation of the CCID experimental design

3. MODELING AND PREDICTIONS

3.1 Data preparation

In this section, two machine learning models are developed to describe how the variation in electrode manufacturing parameters influences the properties and quality of intermediate and final products. The first model is M2S (manufacture to structure), aimed at exhibiting the effect of comma bar gap (*um*), web speed (*m/min*) and coating ratio (%) on thickness (*um*), porosity (%) and dry mass loading (g/m^2) of cathode coating. These parameters are associated with the calendared electrode, where the calendaring step free parameters are kept the same for all cases. The purpose is to focus on coating process and reduce the complexity of models.

The second model is S2P (structure to performance) aimed at correlating capacity (*mAh*) at C/20, C/2, 1C, and 2C rates with thickness (*um*), mass loading (g/m^2) and porosity (%) of assembled half-cells. In total there exists 32 records of experiments addressing the parameters and properties of cathode manufacturing for M2S model and 115 records of performance properties for half coin-cells for S2P model. Figure 5 is the flow diagram of all steps and the input-output sets of each model in this methodology.

It is worth mentioning that after each run of experiments a large piece of electrode/cathode coating is obtained that can be as long as 10 meters in length. However, only a very small section of each piece is used for manufacturing the half coin cells. Therefore, while each thickness, mass loading and porosity data-point in M2S model is an average of all measured values from various locations on the manufactured surface, the thickness and mass loading in S2P is the exact and single measurement related to each small section used for half coin cell assembly as described in 2.3.

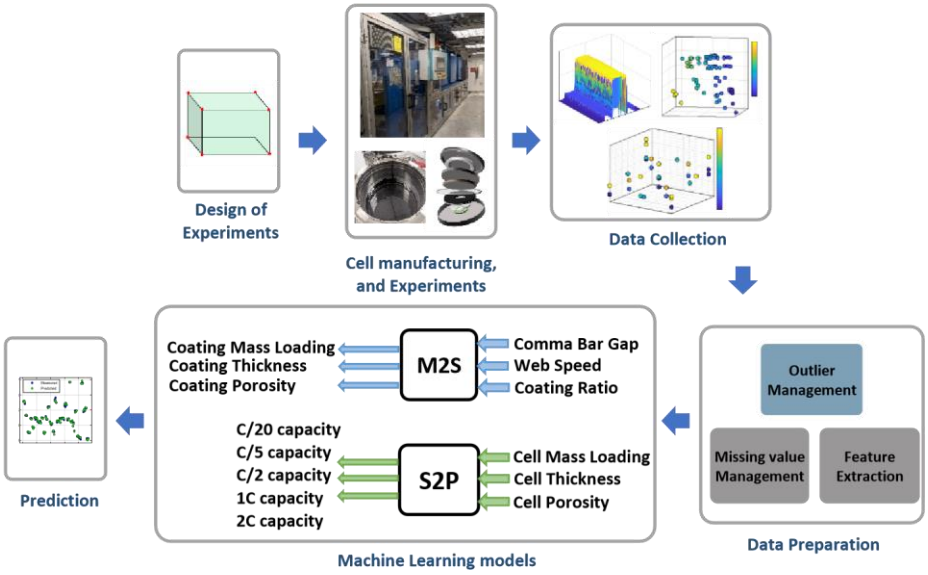

Figure 5 Methodology workflow for manufacturing line modelling and predictions

Since the long piece of the electrode can have nonuniformities, and quite different features at different locations on it, the average coating thickness, mass loading and porosity are not necessarily consistent with these features of the cathode inside each coin cell. Therefore, to minimize the effect of coating nonuniformity on the model performance and its predictability, the two models are trained individually and combining those is under investigation for future works.

The data available via experiments were gone through a data preparation step before being used for M2S modelling as shown in the flowchart of Figure 5. In the first step, the recorded data of the coating mass load as well as thickness and porosity were cleaned from outliers. Outliers were data records at least three times of the scaled median absolute deviations away from the median of all the records at the same experiment. For mass loading outliers were also datapoints related to the edges of the electrodes which were not used for cell assembly later on. For mass loading data, one extra step of missing-value management was followed as well. The reason was that the mass loading data were obtained by continuously measuring the weight over time and position intervals and included various missing records because of errors

of the measurement equipment. These missing values were replaced with the nearest neighbour value to preserve the consistency. In the next step, the features (mean value) of coating mass loading, thickness and porosity were calculated.

The pre-processing steps for all half-cell performance characteristics, as well as half-cell mass loading, thickness, and porosity of S2P model was only limited to outlier removal as the records were directly used as inputs and outputs of the model.

3.2 Modelling and validation Algorithms

In order to predict the intermediate and final product KPIs, support vector regression (SVR) model is trained based on the data. SVR is based on the same concepts of support vector machine for continuous targets. This algorithm is selected because of certain advantages supported by relevant literature such as (Ma & Guo, 2014). It facilitates optimizations by quadratic programming with a global solution. SVR is a soft margin learning method with high robustness to outliers, it is suitable for small sample size and able to transfer a low dimensional nonlinear problem to a high dimensional linear one via kernel trick (Shawe-Taylor & Cristianini, 2004). The goal in SVR is to find a function in training step that can correctly predict the new targets not been considered during training.

To estimate a continuous function *f* with weight *w* and bias *b*, given a multi-dimensional data *x* and *y with N* observations, the problem is first written in the form of (4).

$$y = f(x) = w^T x + b, \quad x, w \in \mathbb{R}^l, \; y, b \in \mathbb{R} \tag{4}$$

For M2S model, *x* includes sample points of the comma bar gap, web speed and coating ration, and *y* includes thickness, porosity, and mass loading of electrodes. On the other hand, for S2P model, *x* consists of cell thickness, porosity, and mass loading and y includes capacity at various C-rates. Solving the estimation problem by SVR is attempted such that, i) the function *f* be as flat as possible which is formulated as (5) which minimizes the norm value or magnitude of *w*, and ii) the distance between the predicted and real outputs is bounded by a prescribed value of *ε* as (6). By this definition of error function, the SVR and be called *ε*-SVR.

$$\min_w \frac{1}{2}\|w\|^2 \tag{5}$$

$$\left| y_n - \left(w^T x_n + b\right) \right| \le \varepsilon, \; n \in N \tag{6}$$

In order to increase the feasibility of the optimization problem, (5) is modified by two non-negative variables *ξ* and *ξ** to achieve a soft margin estimation. By soft margin approach (5) and (6) would reformulate the estimation problem as (7).

$$J(w) = \frac{1}{2}\|w\|^2 + C\sum_{n=1}^{N}\left(\xi_n + \xi_n^*\right) \tag{7}$$

$$s.t. \; y_n - \left(w^T x_n + b\right) \le \varepsilon + \xi_n, \; n = 1, \ldots, N$$

$$\left(w^T x_n + b\right) - y_n \le \varepsilon + \xi_n^*, \; n = 1, \ldots, N$$

$$\xi_n \ge 0, \; \xi_n^* \ge 0$$

Here *C* is the regularization parameter or penalty factor which is for penalizing the training samples that fall outside the margin of ε to avoid overfitting, larger *C* gives more weight to minimizing the prediction error compared to the flatness of function. In order to solve the optimization problem given above, the Lagrange dual formula (8) is used which provides a lower bound for the main optimization problem of (7). The results of two problems do not need to be equal, but the solution of the primal problem would be obtained from the solution of the dual problem (Awad & Khanna, 2015).

$$L(\quad)\square = \frac{1}{2}\square_{i=1}^{N}\square_{j=1}^{N}\left(\square\square\square\square_i - {}_i^*\right)\left({}_j - {}_j^*\right)Gxx\left({}_i, {}_j\right) + \square\square_{i=1}^{N}\left(\square\square_i + {}_i^*\right) - \square_{i=1}^{N} yi\left(\square\square_i - {}_i^*\right) \quad (8)$$

$$st.\ .\ \square_{nN=1}\left(\square\square_n - {}_n^*\right) = 0$$

$$0 \square\square\square_n\ C, 0 \square\square\square_n^*\ C$$

23 Here *G* is the kernel function and *α* is the nonnegative Lagrange multiplier. Kernel functions facilitate mapping data 24 into a higher dimensional space, the kernel space, via them SVR can provide an acceptable accuracy for data with nonlinear 25 interconnections (Shawe-Taylor & Cristianini, 2004). The models in this study are based on quadratic kernels and are 26 compared with the models with linear, cubic, and Gaussian (radial basis) kernels.

27 By dual formula (8), the prediction function can be obtained as (9). The complementary modified conditions required 28 to obtain the optimal solution via dual formula are as (10).

$$f(x) = \sum_{i=1}^{N} (\alpha_n - \alpha_n^*) G(x_n, x) + b \quad (9)$$

$$\alpha_n (\varepsilon + \xi_n - y_n + f(x_n)) = 0$$

$$\alpha_n^* (\varepsilon + \xi_n^* + y_n - f(x_n)) = 0 \quad (10)$$

$$(C - \alpha_n)\xi_n = 0, \ (C - \alpha_n^*)\xi_n^* = 0$$

To handle this optimization problem, it is expressed in the form of quadratic programming and solved by the sequential minimal optimization (SMO) approach (Fan, et al, 2006). SMO is an iterative algorithm based on the optimization of the smallest sub-problem. In each iteration the problem is broken to a set of the smallest sub-problems for SVR, which involves two points and has two Lagrange multipliers of α_i. The Lagrange multipliers are then solved analytically (Platt, 1998).

The model when received a set of training data obtained from experiments, provides M2S and S2P models that can assign predicted electrode and cell KPIs to a similar dataset, i.e., test data set. It's the test dataset that shows the models' ability to predict. Generally, the test data are a fracture of the whole data and obtained by randomly splitting data to train and test. However, considering the fact that in real manufacturing and especially pilot-scale studies the size of data might be rather small, having access to enough data for validation and test can be quite a challenge. To address this issue, here, cross validation (CV) approach is utilised (Fushiki, 2011). CV is both to make a decision about the applicability of a designed model to new data and tuning its hyperparameters. In this approach the data are randomly split into *K* (here, 5) mutually exclusive subsets or folds of the same size. At each run, *K*-1 groups are used for training, and one is left for hyperparameter tuning and test, then, model performance is assessed via an accuracy index. The training and test process is repeated *K* times changing the data used for training and testing until all data go for training and test at least once. Finally, *K* accuracy indices will be available, and their mean and standard deviation represent the final accuracy of the model. *K*-fold cross validation helps taking the risk of over/under fitting into account as well as choosing the tuning parameters of the prediction algorithm systematically. In this approach the best tuning parameter is the one that minimizes the mean squared error (MSE) of fold's predictions i.e., cross validated MSE. The flowchart of the SVR algorithm with cross validation is given in Figure 6.

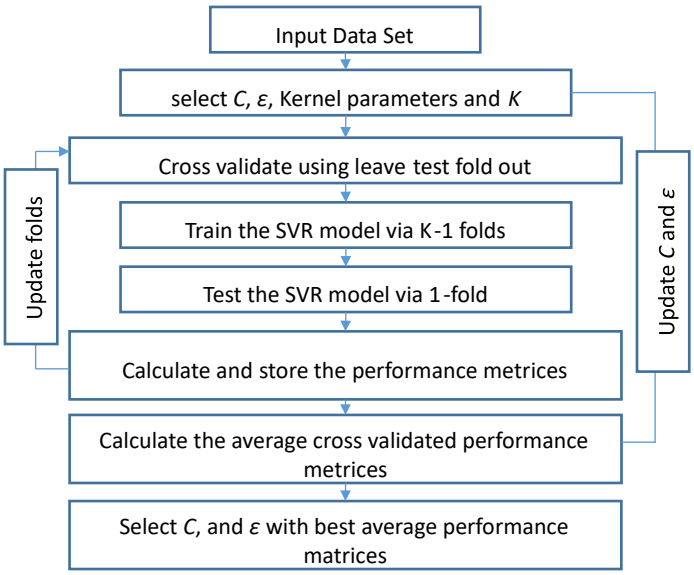

Figure 6 The flowchart of SVR algorithm

4. RESULTS AND DISCUSSIONS

4.1. Structural characteristics and performance Prediction

Based on the experiments, the manufacturing parameters of comma bar gap (um), coating ratio (%) and web speed (m/min) affect the coating thickness, mass loading and porosity. Given the mass loading and the coating thickness, the coating porosity has been calculated by equations (1) – (3). Figure 7 shows the distribution of manufacturing settings in relation to structural properties of battery cathode.

According to these figures a higher dry mass loading is achieved when the comma bar gap is larger and coating ratio is set to a higher value. This is because a larger amount of active material is transferred to the electrode foil in this case. The dependency of mass loading on web speed is not as strong as the other two parameters, suggesting that web speed does not significantly affect the coating weight. For coating thickness, thicker electrodes are obtained by both larger values of comma bar gap and the higher coating ratio. The dependency is justified similar to the mass loading, as with higher values of these two parameters more material is transferred to the electrode surface during manufacturing. Thickness is also higher for slower coating speed. The porosity of the coated electrode has an inverse relationship with the three parameters. At higher values of comma bar gap the porosity decreases as more material is pressed on the surface. This is also the case for web speed and faster coating leaves more pores in the coating.

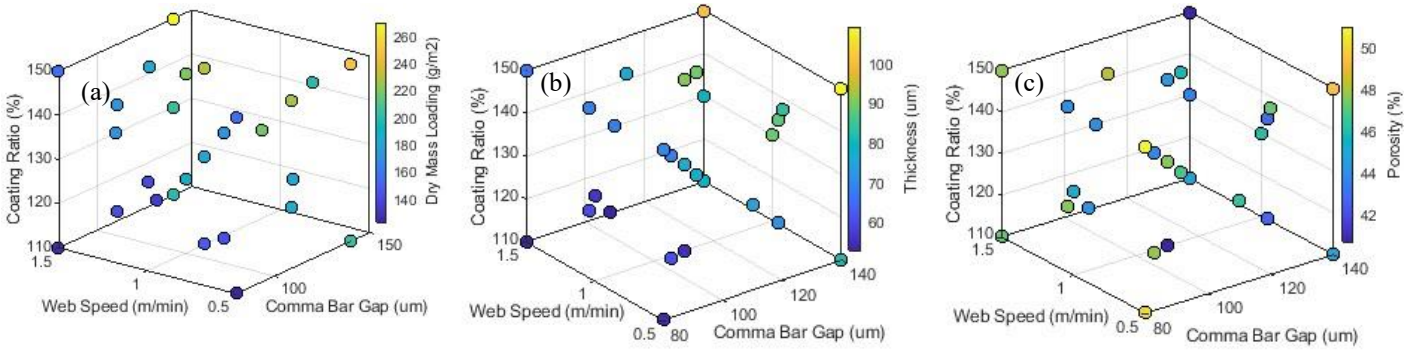

Figure 7 Distribution of manufacturing parameters with relation to (a) dry mass loading, (b) coating thickness, (c) Coating porosity

Similar to the Figure 7, the colour maps of Figure 8 show the distribution of energy capacities at different C-rates in relation to the structural parameters.

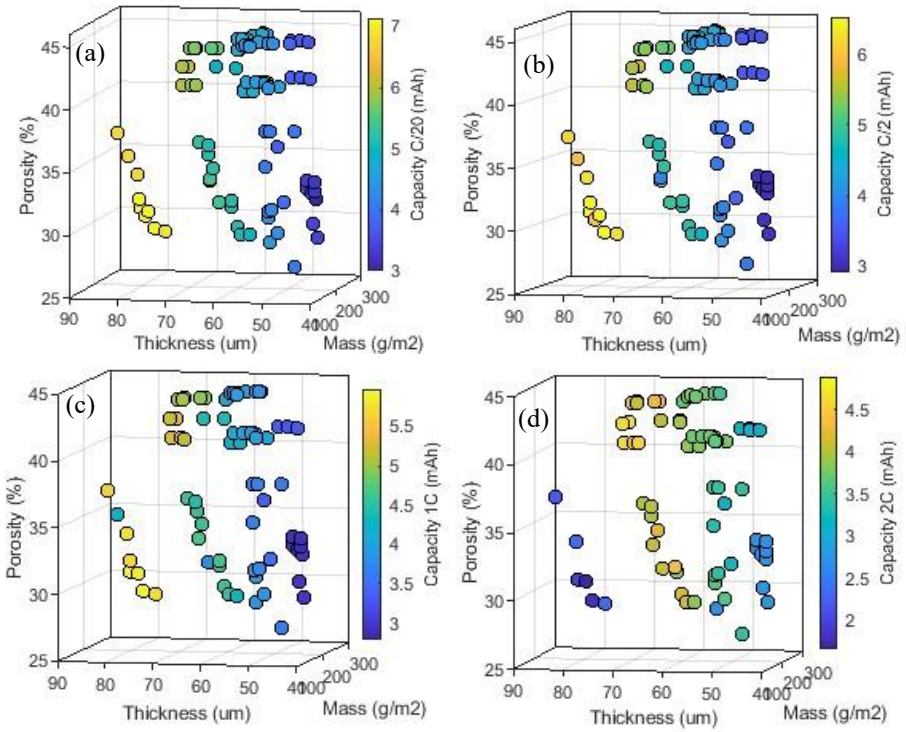

Figure 8 Distribution of the battery structural properties (Mass loading, Thickness and Porosity) with half coin cell performance, (a) Capacity C/20, (b) Capacity C/2, (c) Capacity 1C, (d) 2C

According to the figures, higher thickness, and larger mass loading result cells with higher capacities at C/20, C/2 and 1C C-rates at all porosities between 25% to 45%. This is due to the larger amount of active material that becomes available for the electrodes in these cases. However, for 2C capacity it's the opposite at almost all porosities in the same range. Generally, at higher C-rates, capacity is limited by electronic conduction in the solid components and/or ionic conduction in the pores of the electrode and accordingly for heavier and thicker electrodes the capacity drops off. These general conclusions correspond well with previous studies reported in the literature (Mei, Chen, Sun, & Wang, 2019; Horváth, Coelho, Tian, & Nicolosi, 2020).

Although the figures show a clear dependency between manufacturing and structural parameters with the quality of electrodes and cells, predicting the outputs of each structural and electrochemical properties and quantifying the correlations requires investigation followed in this section. For this purpose, the M2S model is designed to have the three manufacturing inputs and 3 targets. Figure 9 shows the predicted coating features with respect to the associated measured values as well as the prediction error. Each model has been evaluated 10 times, each time by shuffling the data randomly and averaging the results to achieve more confident and statistically reliable conclusions.

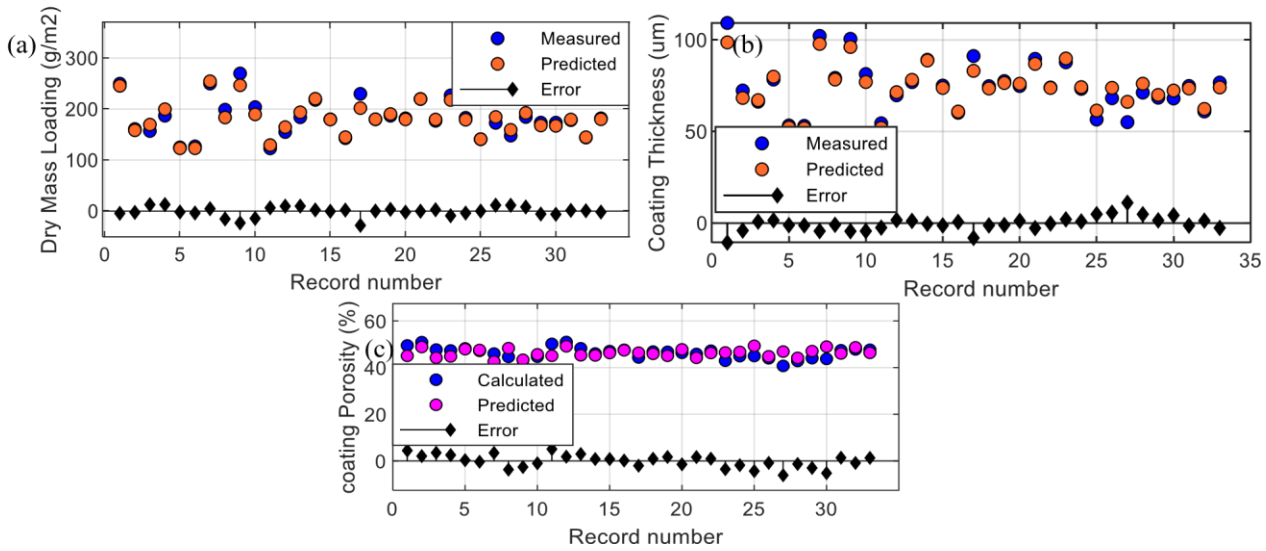

Figure 9 Prediction of cathode structural properties, (a) Mass loading, (b) Thickness, (c) Porosity via M2S model

Similarly, the prediction results for S2P model are depicted in Figure 10. To better visualise the deviation of the predicted results for the data samples in this model, plots for predicted versus actual values are also given. In a representative model, the observations should be very close to the perfect prediction line. According to the figures, most of the predicted targets agree with the observations and cluster around the perfect prediction line without large outliers. This implies the ability of models to capture the pattern of data.

The accuracy of the models is related to the error of predicting the output that is associated with certain input data that has not been used for training but only for validations at each step of cross validation. The accuracy indices here are RMSE defined by $RMSE=\sqrt{\frac{1}{N}\sum_{i=1}^{N}(y_i-\hat{y}_i)^2}$, as well as R^2 and their standard deviations. R^2 is called the coefficient of determination and indicates the proportionate amount of variation in the target variable that has been explained by the independent input variables of the model. It is considered to be a measure of explained variance in relation to the total variance. The larger values of R^2 confirm that more variability has been captured by the model.

R^2 is calculated as $R^2=1-\frac{SSE}{TSS}$ *where* SSE is the sum of the squared error defined as $SSE=\sum_{i=1}^{n}(y_i-\hat{y}_i)^2$. TSE is the total sum of squares obtained via $TSE=\sum_{n=1}^{N}(y_n-\bar{y})^2$, $\bar{y}=\frac{1}{N}\sum_{n=1}^{N}y_n$ for $i=1,\ldots,N$. Beside the two mentioned metrics, mean absolute error (MAE) is also considered as an accuracy measure which is obtained by $MAE=\frac{1}{N}\sum_{i=1}^{N}|y_i-\hat{y}_i|$.

Numeric results of prediction indices are summarized in the Tables 3 and 4. All indices have been reported by their average (mean) value of 10 runs, their standard deviation (std) and percent (%) to the mean value of dataset.

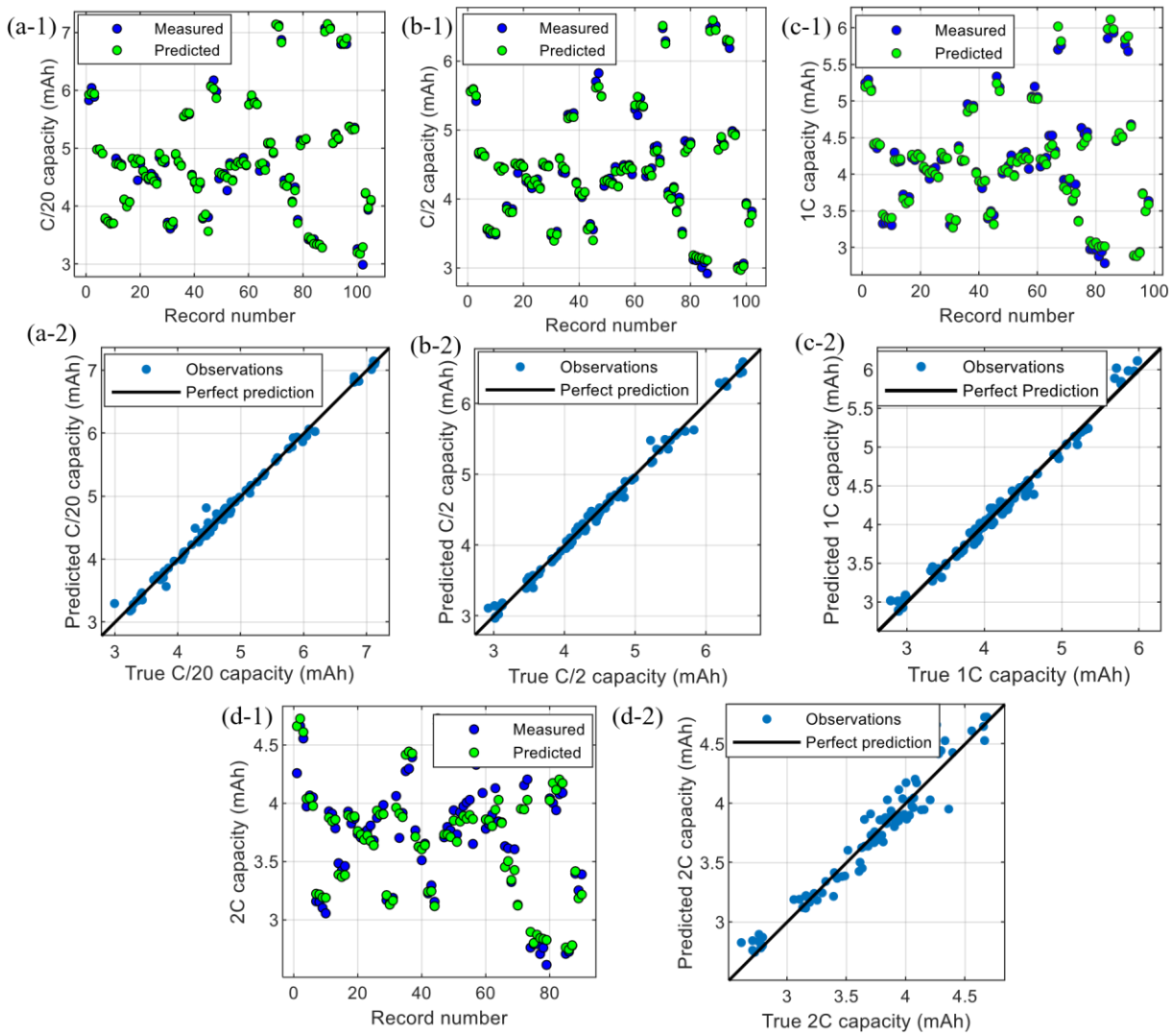

Figure 10 Prediction of half-cell capacity (mAh) (a-1, a-2) C/20, (b-1, b-2) C/2, (c-1, c-2) 1C, (d-1, d-2) 2C through S2P model

Table 3 Prediction performance of three ML methods for Cathode coating Weight and Thickness

Mass Loading							(g/m^2)
Algorithm	RMSE (Mean)	RMSE (Mean %)	RMSE (std)	RMSE (std %)	MAE (Mean)	MAE (%)	R^2 (mean)
SVR	9.33	5.12	0.45	0.2	5.23	2.87	0.94
LR	9.45	5.19	0.46	0.2	7.05	3.87	0.92
DT	21.6	11.8	2.68	1.4	9.55	5.24	0.61
GBT	10.3	5.68	0.53	2.9	9.40	5.16	0.87
NN	9.28	5.10	0.46	0.2	5.15	2.83	0.95
Thickness (*um*)							
Algorithm	RMSE (Mean)	RMSE (Mean %)	RMSE (std)	RMSE (std %)	MAE (Mean)	MAE (%)	R^2 (mean)
SVR	4.03	5.40	0.12	0.1	2.50	3.35	0.92
LR	4.24	5.68	0.18	0.2	3.24	4.34	0.91
DT	9.66	12.9	0.40	0.5	4.15	5.56	0.50
GBT	4.16	5.57	0.21	0.2	3.10	4.15	0.85
NN	4.02	5.39	0.14	0.1	2.21	2.96	0.93

The results are for SVR with quadratic Kernel and compared to four other models including linear regression, decision tree, gradient boosted trees, and feedforward neural network. Linear regression is selected as it usually acts as a benchmark and reference in many regression problems because it is simple to implement and has a low computational cost. Here it is a choice to confirm whether moving from simple linear estimation towards a more advanced model such as the SVR, which is known to be more expensive algorithm in terms of computational cost, is necessary or not. It is also selected to investigate which of the KPIs are linearly predictable and quantify that predictability. The second model is a decision tree, and it is selected as an example of a nonlinear regression model to highlight the performance of SVR particularly with nonlinear kernels. Decision trees are known to be more sensitive to outliers and noise compared to the SVR while less expensive from the computational cost point of view (Suthaharan, 2016; Rokach & Maimon, 2007). Comparisons to decision trees are provided to quantify the performance and run time and investigate whether this nonlinear model could be choice for predicting the KPIs of the battery manufacturing problem.

The SVR is also compared with two advanced models. One is a feed forward neural network, which is a multi-layer perceptron model to investigate if a network of nonlinear functions improves the predictability. The final model is a gradient boosted machine which is a class of ensemble machine learning models. Here the model is based on decision trees so it's a gradient boosted trees model. This model is selected to investigate if advanced techniques such as ensembling could benefit the regression tasks.

Table 3 summarises the results of M2S model. For porosity the results are given separately in Table 4. Since porosity has been calculated based on mass loading and thickness predictions, only RMSE and its deviations are reported.

According to the results of in Table 3 and Table 4, all five M2S models are acceptably accurate. For predicting the mass loading, SVR is resulting a 5.12% error equivalent to 9.33 (g/m^2), the thickness prediction error is about 5.4% or 4.03 (um), both error values are quite small compared to the average weight of a coated electrode. For both targets R^2 is higher than 0.9 which confirms that the model has captured the variability in the data set successfully. Due to the high predictability of these characteristics, the porosity can also be obtained with an error of 5.6%. For all models, the standard deviation of the RMSE is below 0.3%, which shows a high confidence of the reported numbers.

Table 4 Prediction performance of three ML methods for Cathode coating Porosity

Porosity (%)						
Algorithm	RMSE (Mean)	RMSE (Mean %)	RMSE (std)	RMSE (std %)	MAE (Mean)	MAE (%)
SVR	2.63	5.60	0.15	0.3	2.41	5.13
LR	2.74	5.26	0.75	0.1	2.53	5.39
DT	4.85	10.3	0.63	1.3	3.02	6.43
GBT	3.54	7.54	0.56	1.2	3.20	6.81
NN	2.70	5.75	0.22	0.4	2.51	5.34

The RMSE and R^2 values for S2P model are in Table 5 and confirm the ability of the SVR model to predict the half-cell capacity. For lower C-rates of C/20 and C/2, the prediction error is below 2% and R^2 is higher than 0.99. For medium C rate of 1C, the accuracy is 2.5% with R^2 higher than 0.97 and for 2C it is 3.1% with R^2 of 0.97.

Table 5 Prediction error of five ML methods for battery properties

Algorithm	RMSE (Mean)	RMSE (Mean %)	RMSE (std)	RMSE (std %)	MAE (Mean)	MAE (%)	R_2	RMSE (Mean)	RMSE (Mean %)	RMSE (std)	RMSE (std %)	MAE (Mean)	MAE (%)	R_2
	C/20 capacity (*mAh*)							1C capacity (*mAh*)						
SVR	0.075	1.59	0.001	0.02	0.073	1.54	0.992	0.104	2.50	0.002	0.048	0.086	2.0	0.979
LR	0.072	1.53	0.001	0.02	0.072	1.52	0.993	0.104	2.50	0.002	0.048	0.089	2.1	0.978
DT	0.168	3.56	0.036	0.07	0.078	1.65	0.964	0.158	3.80	0.017	0.042	0.091	2.1	0.956
GBT	0.071	1.50	0.001	0.02	0.072	1.52	0.993	0.098	2.36	0.019	0.046	0.078	1.8	0.980
NN	0.073	1.55	0.001	0.02	0.057	1.53	0.993	0.097	2.33	0.010	0.024	0.068	1.6	0.990

	C/2 capacity (*mAh*)							2C capacity (*mAh*)						
Algorith	RMSE (Mean)	RMSE (std %)	RMSE (%)	RMSE (std)	MAE (std %)	MAE (Mean)	R_2	RMSE (Mean)	RMSE (std %)	RMSE (%)	RMSE (std)	MAE (%)	MAE (std)	R_2
SVR	0.071	1.61	0.004	0.09	0.064	1.45	0.993	0.127	3.10	0.007	0.17	0.114	2.78	0.976
LR	0.074	1.68	0.001	0.02	0.065	1.47	0.992	0.289	7.05	0.009	0.20	0.214	5.22	0.874
DT	0.161	3.65	0.034	0.76	0.101	2.29	0.961	0.269	6.56	0.037	0.90	0.206	5.02	0.882
GBT	0.065	1.47	0.001	0.05	0.060	1.36	0.994	0.125	3.05	0.019	0.46	0.101	2.46	0.985
NN	0.066	1.50	0.002	0.04	0.062	1.41	0.994	0.124	3.02	0.020	0.49	0.095	2.32	0.991

The standard deviation of the reported results is very small for all cases with SVR, an RMSE (std%) of 0.02% for C/20, 0.08% for C/2, 0.048% for 1C and 0.17% for 2C shows that for all 10 runs of the model, the RMSE values cluster around the RMSE (mean) very well and the results are highly trustable. In all cases the SVR model performs very well in capturing the pattern of data and can be widely used to predict the battery capacity given the properties of the coating.

Compering the SVR with LR and DT shows that for both S2P and M2S models, the SVR has better performance considering RMSE, its standard deviation as well as R^2. For mass loading, thickness, and porosity, LR is slightly behind the SVR, but DT is significantly weaker. In S2P model, the same trend is noticed between SVR, LR and DT, for capacity in low and medium C-rate, while for higher C-rate of 2C SVR is significantly better than the other two. For both models SVR has the lower standard deviation in the RMSE index, which confirms that SVR has a higher robustness to the organisation of data compared to LR and DT. The superiority is a result of SVR capturing the non-linearity in the data better than LR and DT. It is also because of offering flexibility about the tolerable errors by the model through error margins, it not only minimises the prediction error for training data, but also minimises the upper bound of generalisation error consisting of training error and a confidence level.

Regarding the models of NN and GBT, NN is showing slightly improved accuracy over SVR in the S2P model (0.04 to 0.17% of RMSE). It is also showing slight improvement (0.02% of RMSE) over SVR for M2S model. This is a result of a network structure of this model and its capability of learning more complex and nonlinear patterns of the data set. The gradient boosted tree is having different behaviours for M2S and S2P models compared to other models. This is witnessed in all indices of RMSE, R^2 and MAE. GBT is having a 0.45% to 0.17% higher RMSE for mass loading and thickness but demonstrates an average of 0.1% less RMSE in S2P model outputs. This is believed to be due to the fact that GBT and NN generally require a large dataset for optimising their weight and avoiding overfitting.

In order to complete the comparison between the five models of this study, a comparison between the run time and the computational complexity of models is necessary. Table 6 is developed for this purpose.

In terms of prediction time, the linear regression provides the fastest predictions, and it is followed by DT, GBT, SVR and finally NN. It is worth mentioning that this run time is for equivalent epochs for optimisation. The time is logged by running algorithms on a personal computer with 1.90 GHz and 2.11 GHz CPU and 16.0 GB RAM. The table does not include porosity as it's a direct calculation based on coating weight and its thickness.

Higher run times of NN compared to the others is justifiable considering its more complex structure. Since investigating the effect of electrode's structural parameters on the performance of the battery is usually an offline study and analysis, then the run time of models is not considered as a key factor when selecting a particular prediction algorithm, but definitely it can be a decision-affecting factor for any online analysis of automated manufacturing processes.

Table 6 Run time (sec) of various ML methods for electrode and battery characteristics (single Run)

	SVR	LR	DT	GBT	NN
C/20 capacity	0.205	0.024	0.034	0.136	0.451
C/2 capacity	0.257	0.035	0.038	0.128	0.440
1C capacity	0.225	0.037	0.040	0.131	0.480
2C capacity	0.219	0.046	0.066	0.146	0.442
Coating Weight	0.035	0.021	0.022	0.031	0.490

Coating Thickness	0.029	0.015	0.021	0.028	0.446

4.2 SVR kernel effect on performance

Different kernels affect the generalisation capabilities of the SVR models. To further reflect the predictability achieved via the M2S and S2P SVR models, four different kernels are used to train them and compare the results. With x_i and x_j as the data point, a linear kernel is defined as $G(x_i, x_j) = x_i^T x_j$. A Gaussian kernel is $G(x_i, x_j) = \exp\left(-\|x_i - x_j\|^2\right)$ and a polynomial kernel is given by $G(x_i, x_j) = (1 + x_i^T x_j)^p$ with $p = 2$ for the quadratic and $p = 3$ for cubic cases. The performance of the models is summarized in the Table 7 and Table 8. The best performance of both models belongs to quadratic kernel. For mass loading and thickness in Table 7, if quadratic kernel RMSE values be considered as a benchmark, SVR with cubic kernel leads to 3.4% of more error, while linear and Gaussian kernels are 27.4% and 87.57% less accurate. For capacity prediction at C/20, linear, cubic, and Gaussian kernels result 1.3%, 61% and 89% more error than quadratic kernel, Table 8. For C/2 capacity, linear, cubic, and Gaussian kernels are 4.2%, 55.2% and 64% less accurate. The order slightly changes for 1C and 2C capacities.

Table 7 Kernel effect on SVR model performance for electrode coating properties prediction

SVR	Mass Loading (*g/m2*)		Thickness (*um*)	
Kernel	RMSE	R^2	RMSE	R_2
Linear	11.89	0.811	4.98	0.771
Quadratic	9.33	0.942	4.03	0.92
Cubic	9.65	0.912	4.01	0.887
Gaussian	17.5	0.761	7.70	0.712

Table 8 Kernel effect on SVR model performance for capacity prediction

SVR	C/20 capacity (*mAh*)		C/2 capacity (*mAh*)		1C capacity (*mAh*)		2C capacity (*mAh*)	
Kernel and Index	RMSE	R^2	RMSE	R_2	RMSE	R^2	RMSE	R_2
Linear	0.076	0.993	0.0745	0.992	0.105	0.978	0.260	0.887
Quadratic	0.075	0.992	0.0715	0.993	0.104	0.979	0.127	0.976
Cubic	0.1208	0.981	0.1111	0.982	0.137	0.963	0.145	0.961
Gaussian	0.142	0.985	0.1175	0.987	0.136	0.971	0.147	0.937

For 1C, linear kernel is only 1% less accurate, but cubic and Gaussian kernels are leading to 31% and 30% more errors. Same order is observed for 2C capacity, 1% extra error for linear, and 14% and 15% more error for cubic and Gaussian kernels compared to quadratic kernels. The comparisons suggest that after quadratic kernel, the linear kernel is the best choice, and this is both concluded based on RMSE and R2 values. This would leave cubic and Gaussian kernels out of recommended kernel functions for both of the electrode and half-cell performance prediction purposes.

4.3 Noise Effect (Robustness evaluations)

While the comma bar gap, coating ratio and line speed are set through the coating machine, the other parameters used as the inputs and targets of prediction models are obtained through direct measurement. Coating weight, and thickness are measured via equipment, porosity is calculated via equations, and energy capacities from different half-cells are recorded by cycling tests. All of these observations are subject to measurement noise. Generally, measurement noise is an inevitable part of data at real manufacturing scale. In fact, different manufacturers might not have access to costly and very accurate sensors. Therefore, it is important to evaluate the robustness of the models so that the manufacturers can decide whether it is applicable to them with the level of noise in their data. The measurement noise if considered in the training step, the resilience of the model would be increased and the predictions will be more reliable for the validation data (Isaev & Dolenko, 2018). In order to analyse the robustness of model, three steps have been taken here. First the training data are augmented to include measurement noise. This is achieved by intentionally adding a fixed level of noise and creating a synthetic data set based on the original data, the approach is adopted from (Xu, Caramanis, & Mannor, 2014). The noise is assumed to be of Gaussian type with a variance between [1 -10] % of sample records while preserving the mean value of them. Then, the models are trained for the data and validated by 5-fold cross validation approach. Finally, the robustness of models to noise level is evaluated by both the RMSE (%) of the average predicted variable as well as the R^2 coefficient.

The Figure 11 and Figure 12 show the error level, in % of data that has been used to augment the data, versus the RMSE and R^2. Here, an acceptable model is defined to have less than 15% RMSE, (blue region) and R^2 higher than 0.7 (red region), these threshold are adjusted following the definition of a predictive model in (Tropsha, et al, 2003). The vertical overlap of two regions, (RMSE < 15% and R^2 > 0.7) shows the upper limit of noise which is tolerable by models.

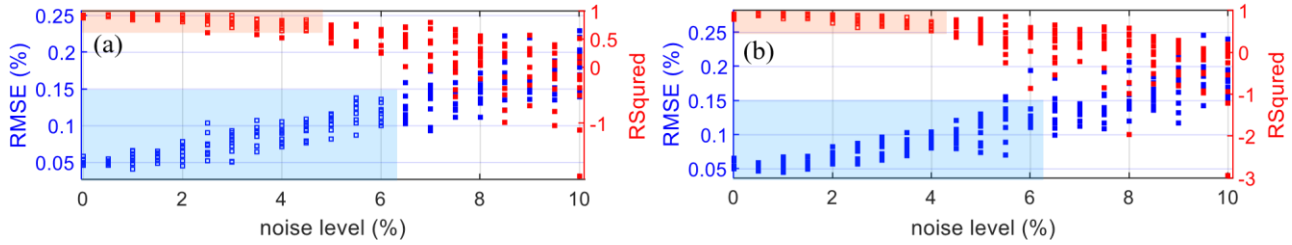

Figure 11 M2S SVR Robustness to noise analysis, (a) Mass load, (b), Thickness

Figure 11 is devoted to M2S model for predicting coating mass load and thickness. Similarly, Figure 12 shows the dependency of the RMSE and R^2 values to the noise level in the data set of S2P model.

It is worth noting that models are run 10 times for capturing the variation in performance metrics and the effect of random noise added to the data. The noise level has been incremented by 0.5% for all models. The results at location 0 of the x axis of each figure show the model performance of original data. Compared to location 0, original data scenario, noise in data increases the prediction error and reduces the R^2 value. This is accompanied by an increase in the variance observed for both metrics due to an increase in the variance of noisy data.

Figure 11 implies that the M2S can tolerate measurement noise up to 6.5%. Same level of noise is tolerable by M2P as well. According to Figure 12, while the prediction RMSE can be in the acceptable range of [0 -15] % for up to 9% of the noise, the R^2 drops below 0.7 after increasing the noise to only 6.5%. This concludes that despite the presence of noise in the data, the predictability of SVR model can still be maintained up to a good level.

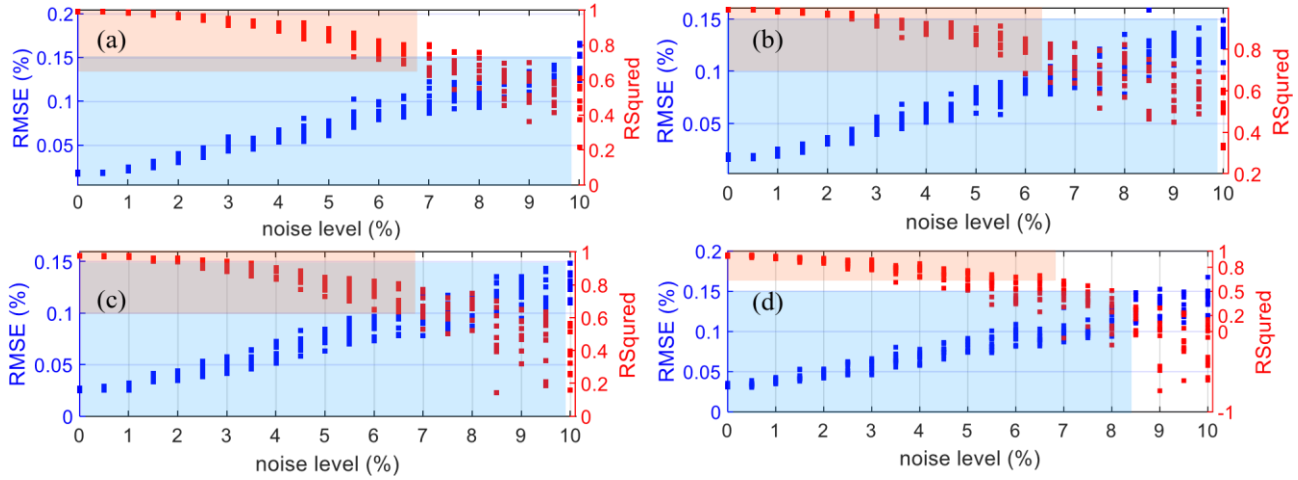

Figure 12 SVR Robustness to noise analysis, (a) C/20 capacity, (b), C/2 capacity, 1C capacity, (d) 2C capacity

4.4 Training by limited number of input variables

Battery manufacturing process is a complex chain with numerous variables at various steps. Monitoring and measuring all the variables are very costly and not practical in the context of volume manufacturing. Therefore, to understand the significance of each of the input variables for the accuracy of the predicted coating properties and half-cell performance, in this section, SVRs are trained with a limited number of predictors. The results of each attempt are then compared in terms of RMSE. This analysis is important to understand if one or more of the input variables can be taken out of the input variable pool for a simpler and/or more accurate model, to improve the efficiency of the model development process and underpinning data collection activity.

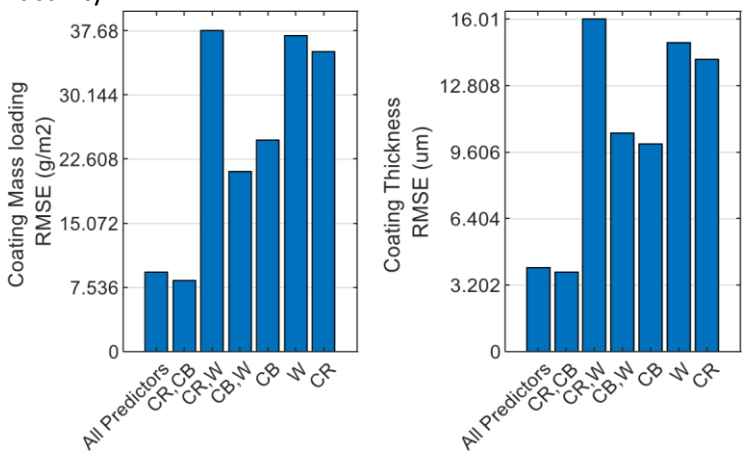

Figure 13 Comparing RMSE in regression by different manufacturing settings as predictors

The comparative results of the M2S model, with the regression index of RMSE, are given in Figure 13 for a selection of the coating ratio (CR), comma bar gap (CB) and web speed (W) inputs. According to these figures the lowest error is achieved with the pair of comma bar gap and coating ratio as the predictors.

The regression indices for S2P model are also given in Figure 14. Considering the results, it can be concluded that for C/20 capacity, C/2 capacity and 1C capacity, the single input of mass loading (M) can provide results as accurate as all inputs.

This means that for low and medium C-rates, the capacity is more dependent to mass loading and less to the thickness (T) and porosity (P). However, the RMSE values for 2C capacity confirm that neither of inputs by their own are enough for understanding the pattern of data and all three inputs are required to capture the variance in the data and make a successful prediction.

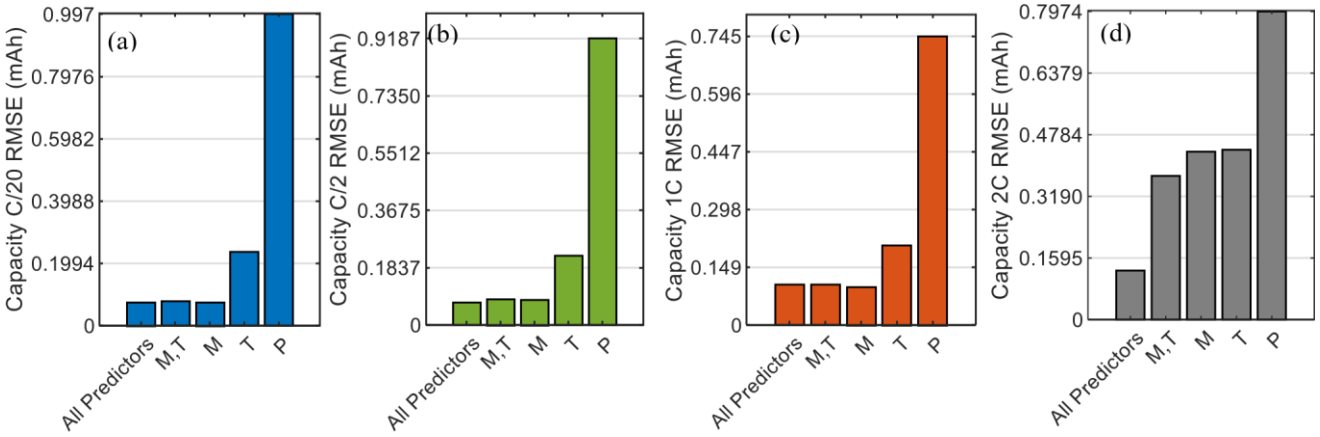

Figure 14 Comparing RMSE in regression by different structural properties, (a) C/20 capacity, (b), C/2 capacity, (c) 1C capacity, (d) 2C capacity

To further analyse the impact of each input variable on the electrode and cell characteristics, correlation coefficients between any two pairs are calculated via Pearson product-moment correlation coefficient formula (Cleophas & Zwinderman , 2018).

Correlation coefficients are values between 0 and 1 and can be positive or negative. A positive coefficient for a pair of variables implies a direct relationship between those pair and means increase in one variable would increase the other. Also, the larger the number the stronger the correlation. When a correlation coefficient is 1 it means that the two variables are linearly related.

According to the heatmap Figure 15 (c) for M2S model, comma bar gap, web speed and coating ratio are fairly independent and only minor correlations is noticed in between those. For S2P model, the thickness and mass loading are strongly correlated, Figure 15 (d). Both coating weight and thickness are highly correlated with the manufacturing parameters of coating ratio and comma bar gap, Figure 15 (a) and this is exactly what was suggested by Figure 13. For S2P model, all capacities at various C-rates are highly correlated with the cell Mass Loading and Thickness. Considering the interconnections between mass loading and thickness according to Figure 15 (d), the importance of mass loading in the prediction of C/20, C/2 and 1C capacities shown by Figure 14 (a), (b) and (c) is justifiable.

The strong correlation between 2C capacity and cell porosity is also confirming its contribution in lowering the prediction error as found by Figure 14 (d). Obviously, there is a different impact of key factors on the capacity at various C-rate. For discharge at 1C and under, the limiting process in the electrode is resistance. Thus, the capacity increases for thicker / higher coat weight electrodes, and the coating porosity has relatively little impact. However, at high rates, the limiting process is usually mass transport, and often ionic conduction of liquid electrolyte in the pores of the electrode. Thinner electrodes perform better than thicker electrodes at very high discharge rates. At 2C, the electrode is arguably in the transitional region between these two limiting processes. For thicker electrodes, there is a conflict between increased capacity and reduced ionic conductivity, and therefore porosity is an important factor and increased porosity is beneficial.

The comparisons for both M2S and S2P models with fewer features show that for larger data sets a selection of the inputs instead of all may be used in order to reduce the complexity of models. In fact, the ability of predicting target

variables with a smaller number of input variables will significantly reduce the costs associated with the measurement of less important inputs.

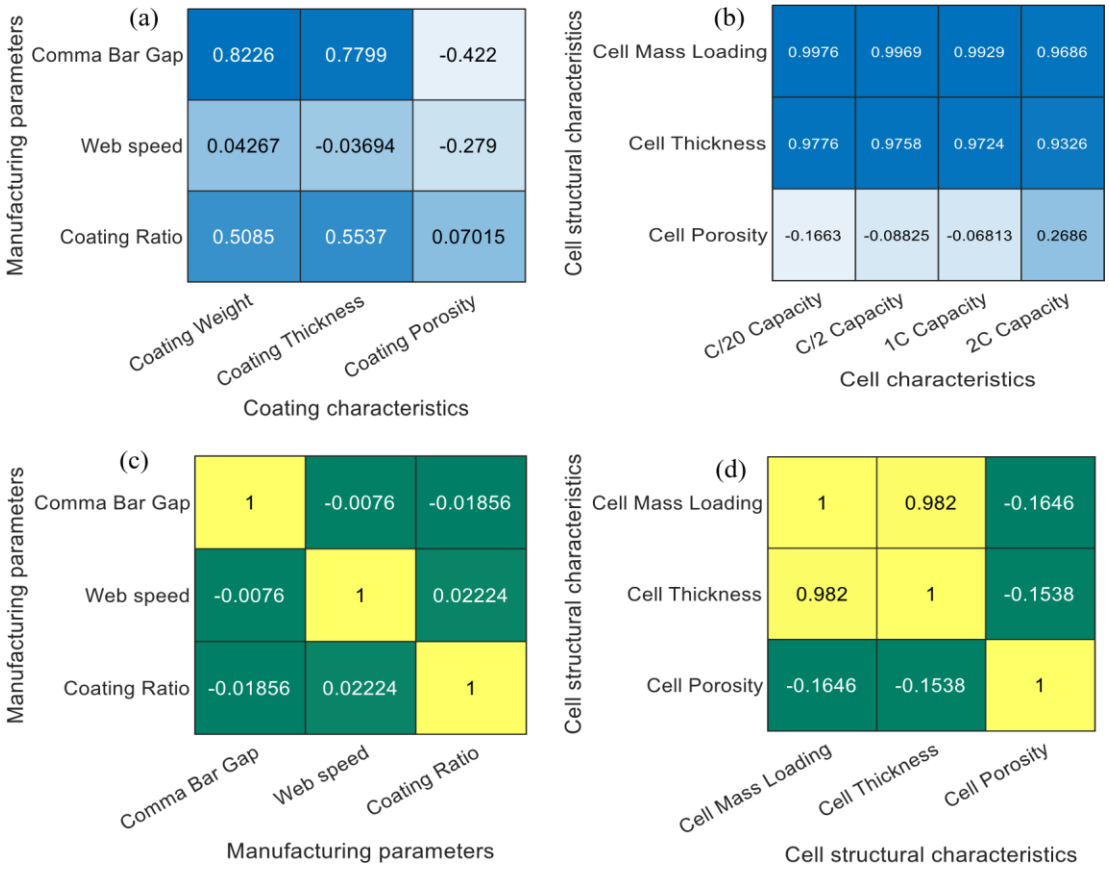

Figure 15 Correlation coefficients for models (a) Input-Output of M2S, (b) Input-Output of S2P, (c) Inputs of M2S, (d) Inputs of S2P

4.5 Effect of K in K-fold validation method

K fold validation is a solution when the size of the dataset is rather small. It is a resampling procedure to give every single sample to be part of both training and testing processes and evaluate model performance. The number of folds, *K*, is a variable that can be selected arbitrarily. Generally, when *K* increases the size of the training subset grows and the size of the test subset becomes smaller in each try. Also, by an increased *K*, the difference between the training and resampling subsets becomes smaller. As this difference decreases, the bias of the modelling technique reduces. This is achieved at the cost of higher variance of the model performance index obtained from multiple (*K*) tries. Empirically, two common choices of *K* are 5 and 10, which have shown to provide validation error estimates with an acceptable balance between bias and variance. Here, Table 9 and

Porosity is not included in the M2S table as it is calculated based on predicted values of the other two variables. Some of the indices of the given tables are visualised in Figure 16.

Table 10 are given to highlight the effect of *K* on the M2S and S2P model performance based on the battery manufacturing data set.

Table 9 The performance of M2S SVR model under validations with different folds (K)

Coating Weight (g/m^2)	Coating Thickness (um)

Folds	RMSE (Mean)	RMSE (%)	RMSE (std)	RMSE (std %)	R^2	R^2 (std)	Time (mean)	Time (std)	RMSE (Mean)	RMSE (%)	RMSE (std)	RMSE (std %)	R^2	R^2 (std)	Time (mean)	Time (std)
2	10.10	5.54	0.33	0.18	0.884	0.013	0.021	0.011	4.33	5.79	0.07	0.09	0.790	0.012	0.022	0.010
3	10.07	5.53	0.39	0.21	0.896	0.015	0.024	0.012	4.29	5.74	0.10	0.13	0.860	0.0145	0.025	0.012
5	9.331	5.12	0.45	0.25	0.943	0.016	0.035	0.015	4.03	5.40	0.12	0.16	0.921	0.0164	0.029	0.014

10	9.013	4.94	0.51	0.28	0.958	0.030	0.121	0.022	3.93	5.27	0.22	0.29	0.930	0.0370	0.124	0.021
15	8.862	4.86	0.71	0.39	0.961	0.033	0.130	0.036	3.90	5.23	0.29	0.39	0.934	0.0389	0.142	0.038

1

2 Porosity is not included in the M2S table as it is calculated based on predicted values of the other two variables. Some 3 of the indices of the given tables are visualised in Figure 16.

4 *Table 10 The performance of S2P SVR model under validations with different folds (K)*

	C/20 capacity (*mAh*)								1C capacity (*mAh*)							
Folds	RMSE (Mean)	RMSE (%)	RMSE (std)	RMSE (std %)	R^2	R^2 (std)	Time (mean)	Time (std)	RMSE (Mean)	RMSE (%)	RMSE (std)	RMSE (std %)	R^2	R^2 (std)	Time (std)	Time (mean)
2	0.087		1.84	0.0008	0.016	0.991	0.0013	0.163	0.071	0.110	2.64	0.0013		0.031	0.970	0.0004		0.135
3	0.071 0.078		1.65	0.0009	0.019	0.992	0.0015	0.181	0.076	0.106	2.55	0.0021		0.041	0.974	0.0005		0.169
5	0.075		1.59	0.0014	0.029	0.992	0.0021	0.205	0.085	0.104	2.50	0.0023		0.048	0.979	0.0006		0.225
10	0.102		0.074	1.57	0.0021	0.044	0.993	0.0032	0.298	0.102	0.096	2.31	0.0030		0.071	0.982	0.0012	
15	0.470 0.073	0.145	1.55	0.0030	0.063	0.993	0.0034	0.442	0.133	0.094	2.26	0.0042		0.010	0.986	0.0031		0.717	0.181

	C/2 capacity (*mAh*)								2C capacity (*mAh*)							
Folds	RMSE (Mean)	RMSE (%)	RMSE (std)	RMSE (std %)	R^2	R^2 (std)	Time (mean)	Time (std)	RMSE (Mean)	RMSE (%)	RMSE (std)	RMSE (std %)	R^2	R^2 (std)	Time (std)	Time (mean)
2	0.074		1.68	0.002	0.05	0.991	0.003	0.166	0.067	0.139	3.39	0.0056		0.14	0.937	0.0028		0.145	0.065
3	0.076		1.72	0.003	0.07	0.992	0.004	0.193	0.068	0.138	3.37	0.0062		0.15	0.940	0.0031		0.161	0.066
5	0.071	1.61	0.004		0.09	0.993	0.005	0.257	0.092	0.127	3.10	0.0073		0.17	0.976	0.0044		0.219	0.085

10	0.070	1.59	0.005	0.10	0.993	0.007	0.415	0.096	0.119	2.90	0.0083	0.20	0.981	0.0056	0.275	0.087
15	0.069	1.56	0.007	0.16	0.993	0.008	0.685	0.136	0.1157	2.80	0.0096	0.23	0.982	0.0064	0.388	0.105

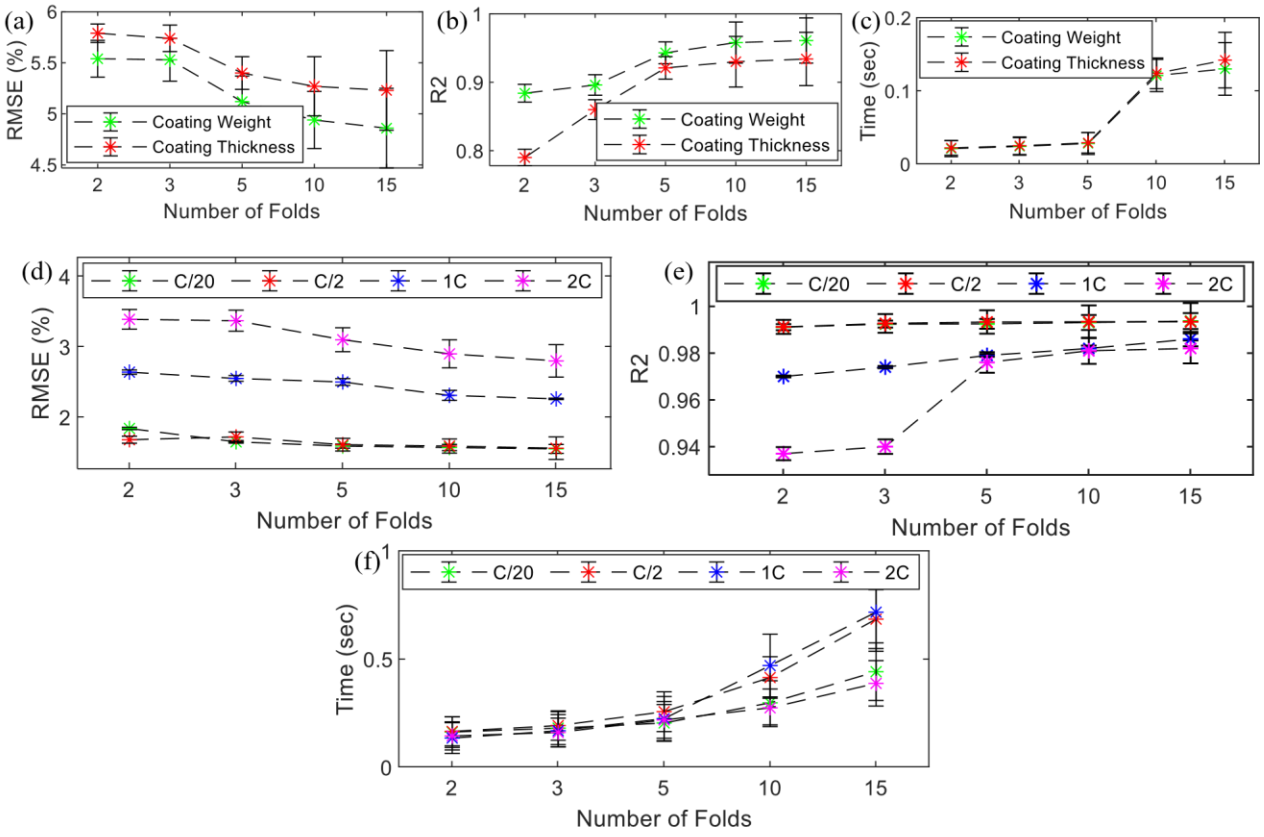

Figure 16 K effect in K-Fold validation of SVR, (a), (b), (c), indices of M2S model, (d), (e), (f), indices of S2P model

According to the figures, as the number of folds increases the error of the validation reduces, Figure 16 (a) and (d), and the R^2 index increases, Figure 16 (b) and (e). This highlights that the bias of the model and the degree of overfitting is reduced with increased *K*. The process time and computational complexity are on the other hand and is a conflicting decision factor when choosing *K*. As shown in Figure 16 (c) and (f), by increasing *K*, the number of training and test processes increases, which causes an increase in the total process time. Considering the conflicting factors, *K* = 5 is a

rational choice for this problem, especially because the improvement rate after this value is rather small considering the complexity of calculations it adds.

4.6 Dataset size effect

In general, the accuracy of predictions based on machine learning is a function of the data size and the richness of data. While a large dataset may improve the accuracy in training phase it may raise concerns about overfitting. One of the questions that needs to be answered before transferring a model from lab scale to volume scale or from one manufacturer to the other is about the size of the data set required to obtain a desirable prediction accuracy. In order to answer this question and quantify the effect of the data size on model performance, in this section SVR models are trained by different fractions of the available data. This study is only conducted for S2P model which has a bigger data set coming from the designed experiments and further analysis for M2S will be performed in future works when more experimental data are available. Figure 17 shows the effect of the number of experiments (samples) on the prediction error of each half-cell battery characteristic. Results are accompanied with the RMSE of linear regression and decision tree to further highlight the SVR methods merits. Similar to the previous sections, all models are trained for 10 selections of data and at each attempt the data are selected randomly from the pool of all data (115 samples).

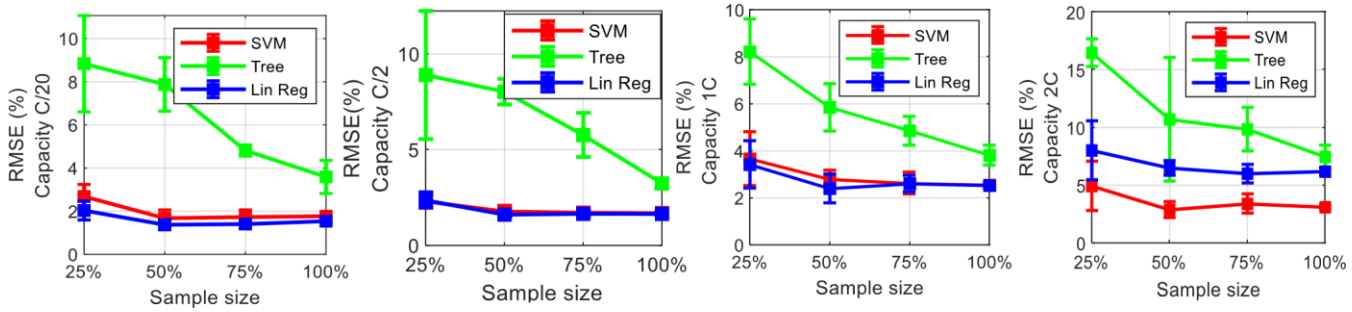

Figure 17 The prediction accuracy in % with respect to the data size (a) C/20 capacity, (b) C/2 capacity, (c) 1C capacity, (d) 2C

According to Figure 17, the model prediction error reduces as the data size increases. The trend is generally visible in all four predicted characteristics. It is worth noting that the decision tree method is showing significantly larger prediction error for energy capacities in all cases. While the accuracy of SVR and linear regression have almost same RMSE trend and reduction slope in response to reduction in data size for C/20, C/2 and 1C capacities, for 2C-rate capacity the SVR is showing the least error for smaller data sets. For all the 4 battery characteristics, SVR is giving accurate results even with small data sets and this is aligned with the findings of previous literature on the data size effect on model accuracy (Tange, Rasmussen, Taira, & Bro, 2017; Cunha, Lombardo, Primo, & Alejandro , 2020). The results suggest that the data size can be reduced in all cases according to the desired prediction accuracy. Obviously, the reduction in data size should be performed only by making sure that the smaller data set can still cover the range of inputs and targets and explain the variation in the data.

4.7 Interpolation between characteristics

As reported in the previous sections, a model trained via the experimental half-cell data with electrochemical characteristics at a specific C-rate can successfully predict the same C-rate capacity given the inputs of mass loading, thickness, and porosity. In this section is it shown that the model can also predict the performance at any other C-rates in between the minimum and maximum C-rates used for training, even if the associated data is not included in the training of the model. For this purpose, the C-rate (cycling current) is considered as the fourth input of the model beside mass loading, thickness, and porosity. Then, the model is trained via energy capacity data at all C-rates expect a particular one and finally that excluded C-rate data is used for validation.

The predicted values and their relation to the true data are given in Figure 18 for three different scenarios. For scenario (a), C/20, C/2, 1C, and 2C data are used for training then C/5 capacity is predicted. The RMSE at this case is 0.128 (*mAh*) which is equivalent to 2.8% error, the R^2 is 0.98. For scenario (b), C/20, C/5, 1C, and 2C capacities are used for training and

C/2 is used for validation. In this case the RMSE is less than 0.128 (*mAh*) or 2.9% with R^2 of 0.97. In the final case, (c), 1C is excluded from the same training data pool and then validated. The prediction error in this case is 0.1502 (*mAh*) or 3.3% with R^2 of 0.97. According to the results, the RMSE for predicting low C-rate capacities is very desirable, even if they are not considered in the training step of building the model. The error for 1C capacity is slightly higher than the other two which is due to its dependency to 2C capacity data that has higher variability compared to the C/20, C/2, and C/5 capacity data.

The part 3 of Figure 18 has summarized the importance of each input in the model performance. According to the results, while C-rate (C) cannot act a as sole input to provide enough accuracy when interpolating the capacities, when used beside the electrode characteristics of mass loading (M), thickness (T), and porosity (P), it can help to predict the target. Figure 18, (a-3), (b-3) and (c-3) also confirm that mass loading, thickness, and C-rate (M, T, C) are the inputs with the most significant impact on the model accuracy.

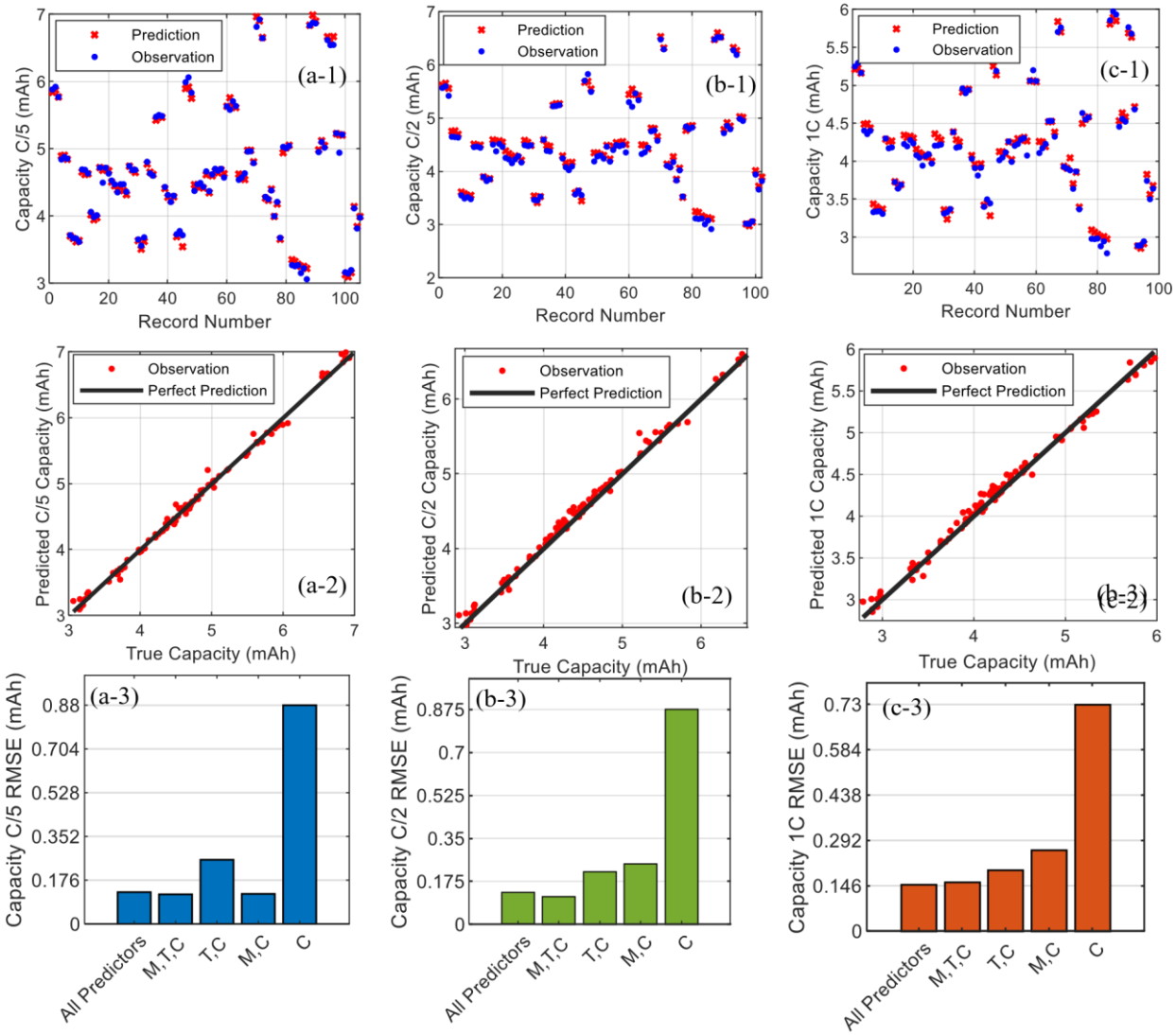

Figure 18 S2P Model capability for Capacity interpolation

The ability of the models with an extra input of C-rate to get capacities at other cycling conditions is a very significant advantage for manufacturers as it will eliminate the need to run experiments in the labs for obtaining that the values. This is more significant at lower C-rates since they can be quite time consuming due to the smaller inputs current applied to cells for discharging purposes.

5. CONCLUSIONS

This study introduces a model-based quality assessment method for the Li-ion battery by analysing its manufacturing process parameters. The purpose is to determine the key parameters affecting the characteristics of the intermediate products during electrode (cathode) coating step and guarantee a desired final cell quality via data-centric analysis.

This work is built upon a case study with 133 Li-ion battery cells manufactured in the pilot line of The University of Warwick (UK). It combines the design of experiments techniques, data acquisition, data preparation, machine learning and artificial intelligence to represent the battery production processes. It is based on a set of input and output variables that have not been studied in the previous literature and suggests a new methodology for model-based prediction of battery characteristics from the manufacturing variables. It is providing opportunities for in-situ control of the manufacturing processes and the ability to:

- Predict battery electrochemical performance, i.e., energy capacity, based on manufacturing variables,
- Define and quantify the correlation between manufacturing parameters and electrode/cell performance,
- Facilitate flexible manufacturing without the need for resource intensive calculations and setups each time the quality targets are changed,
- Perform model-based quality checks where experiments are hardly applicable (e.g., after battery cell assembly),
- Distinguish cells with lower quality or higher probability to fail at earlier stages.

This study paves the way towards optimised battery production with a reduced carbon footprint via limiting the waste of resources due to the failed processes and replacing characterisation tests with model-based predictions.

The analysis during this study revealed that the cathode's structural features are highly predictable, with about 5% error, via the coating manufacturing parameters of comma bar gap, coating ratio and web speed. Among the three selected features for cathode manufacturing modelling, comma bar gap and coating ratio had the most significant effects on the predictability of the model. Correlation analysis showed that the three parameters are highly independent with correlation coefficients weaker than 2%.

The results also showed that half-cell energy capacities are highly predictable with circa 3% error at various loading Crates given cell features of electrode mass loading, thickness, and porosity. Mass loading and thickness were identified as the most important predictors for most of the C-rates, while electrode porosity was also important for predictions at higher C-rate. Thickness and mass loading were detected as strongly correlated features with correlation coefficients higher than 98%. For electrochemical characteristics, the prediction accuracy reduced as the C-rate increased and this was because the environmental variables such as temperature become more significant in the cell performance at higher Crates and introduce more degrees of freedom. The analysis showed that SVR is a better method compared to liner regression and decision trees when dealing with battery manufacturing and performance data, while more advanced machine learning models of artificial neural networks and gradient boosted trees, were at the same levels of accuracy or only about 0.1% more accurate due to the rather small data set. It was also found that SVR can preserve the predictability with a smaller number of data and can tolerate measurement noise up to 6.5%.

To further address the challenges of optimised battery manufacturing, future works are still required. There are four main directions under study by the authors.

1) Models and experiments are sought to be extended in order to predict other the electrochemical characteristics such as internal resistance at various states of charge and gravimetric/volumetric capacity.

2) More manufacturing steps are intended to be taken into account. Here the focus has been on calendared coating parameters, and it is worth considering the mixing and drying step data to reveal the interconnections.

3) Apply methodology and models to anode coating and associated half-cells is another direction to be pursued. Although it is believed that the concepts would be the same, the manufacturing parameters are expected to have different effects on the anode's features.

4) Analysing the transformability of the methods to the full-cell scale as well as other types of cells, such as cylindrical and pouch cells is another area to be investigated more deeply in the future.

APPENDIX

In order to increase the reproducibility of the results reported in this paper, the full list of the model parameters and setting are given here. The hyper parameters of all models have been set via a grid search method and optimisation in the ranges provided as the following:

- Support vector regression: Kernel= [polynomial degree 2 (quadratic), polynomial degree 3 (cubic), Radial basis function, linear], gamma of Gaussian kernel = scale, C = [0.1 1000], ε = [0.01 0.5].
- Neural networks: Number of hidden layers = [5 10], Maximum number of epochs = 50, Training function = LevenbergMarquardt backpropagation.
- Decision tree: Minimum samples split = [2 5], Minimum samples leaf = [1 5].
- Gradient boosted tree: Number of leaves = [2 50], Maximum depth = -1, Learning rate = [0.005 0.5], Number of estimators = [50 2000], Subsample for bin= [20 1000], Minimum child samples= [1 10]. The data of this study could also be shared upon request.

ACKNOWLEDGEMENT

This research was undertaken as part of the NEXTRODE project, funded by the Faraday Institution, UK. Grant Number: FIRG015.

CREDIT AUTHORSHIP CONTRIBUTION STATEMENT

M Faraji Niri: Conceptualization, Methodology, Software, Investigation, Data curation, Formal analysis, Validation, Visualization, Writing - original draft. K Liu: Methodology, Investigation, Writing - review and editing. G Apachitei: Conceptualization, Methodology. L Roman Ramirez: Conceptualization, Methodology. M Lain: Conceptualization, Methodology. D Widanage: Funding acquisition, Supervision. J Marco: Funding acquisition, Supervision, Writing - review and editing.

DECLARATION OF COMPETING INTEREST

The authors declare that there is no known competing financial interests or personal relationships that could have appeared to influence the work reported in this paper.

REFERENCES

Attia, P., Grover , A., Jin, N., Severson, K., Markov, T.M., Liao., Y.H., Chen, M.H., Cheong, B., Perkins, N., Yag, Z., Herring, P. (2020). Closed-loop optimization of fast-charging protocols for batteries with machine learning. *Nature, 578*(7795), 97-402.

Awad, M., & Khanna, R. (2015). *Efficient learning machines: theories, concepts, and applications for engineers and system designers.* Springer nature.

Chen, Y., Duquesnoy, M., Tan, D., Doux, J., Yang, H., Deysher, G., Ridely, P., Franco, A.A., Meng, Y.s., Chen, Z. (2021). Fabrication of High-Quality Thin Solid-State Electrolyte Films Assisted by Machine Learning. *ACS Energy Letters, 6*(4), 1639-1648.

Cleophas, T., & Zwinderman , A. (2018). Bayesian Pearson Correlation Analysis. In *Modern Bayesian Statistics in Clinical Research.* Cham, Switzerland: Springer.

Cunha, R., Lombardo, T., Primo, E., & Alejandro , A. (2020). Artificial intelligence investigation of NMC cathode manufacturing parameters interdependencies. *Batteries & Supercaps, 3*(1), 60-67.

Dahodwalla, H., & Herat, S. (2000). Cleaner production options for lead-acid battery. *Journal of Cleaner Production, 8*(2), 133-142.

Duquesnoy, M., Boyano, I., Larraitz, G., Cereijo, P., Elixabete , A., & Alejandro, F. (2021). Machine Learning-Based on Assessment of the Impact of the Manufacturing Process on Battery Electrode Heterogeneity. *Energy and AI, 5*, 100090.

Duquesnoy, M., Lombardo, T., Chouchane, M., Primo, M., & Franco, A. (2020). Data-driven assessment of electrode calendering process by combining experimental results, in silico mesostructures generation and machine learning. *Journal of Power Sources, 480*, 229103.

Fan, R., Chen, P., & Lin, C. (2006). A Study on SMO-Type Decomposition Methods for Support Vector Machines. *IEEE Transactions on Neural Networks, 17*, 893-908.

Faraji, M., Bui, T., Fai Yu, T., & Marco, J. (2020a). Model-Based End of Discharge Temperature Prediction for Lithium-Ion Batteries. *IFAC-PapersOnLine, 53*(2), 12701-12707.

Faraji, N., Liu, K., Apachitei, G., Roman, L., Widanage, D., & Marco, J. (2020b). Data mining for quality prediction of battery in manufacturing process: Cathode coating process. *International Conference on Applied Energy.* Bangkok.

Faraji, M., Marco, J., Quang Dinh, T., & Fai Yu, T., (2019). Two layer Markov model for prediction of future load and end of discharge time of batteries. *International Conference on Mechatronics Technology* Italy.

Filz, M., Gellrich, S., Turetskyy, A., Wessel, J., Herrmann, C., & Thiede, S. (2020). Virtual Quality Gates in Manufacturing Systems: Framework, Implementation and Potential. *Journal of Manufacturing and Materials Processing, 4*(4), 106.

Fushiki, T. (2011). Estimation of prediction error by using K-fold cross-validation. *Statistics and Computing, 21*(2), 137-146.

Garg, A., Yun, L., Gao, L., & Putungan, D. (2020). Development of recycling strategy for large stacked systems: Experimental and machine learning approach to form reuse battery packs for secondary applications. *Journal of Cleaner Production, 275*, 124152.

Hanisch, C., Schünemann, J., Diekmann, J., Westphal, B., Loellhoeffel, T., Prziwara, P., Haselrieder, W. Kwade, A. (2015). In-production recycling of active ma- terials from lithium-ion battery scraps. *ECS Transactions, 64*(22), 131-145.

He, H., Tian, S., Tarroja, B., Ogunseitan, O., Samuelsen, S., & Schoenung, J. (2020). Flow battery production: Materials selection and environmental impact. *Journal of Cleaner Production, 269*, 121740.

Hong, J., Wang, Z., Chen, W., Wang, L., Lin, P., & Qu, C. (2021). Online accurate state of health estimation for battery systems on realworld electric vehicles with variable driving conditions considered. *2021, 294*, 125814.

Horváth, D., Coelho, J., Tian, R., & Nicolosi, V. (2020). Quantifying the Dependence of Battery Rate Performance on Electrode Thickness. *ACS Applied Energy Materials, 3*(10), 10154-10163.

Isaev, I., & Dolenko, S. (2018). Training with noise addition in neural network solution of inverse problems: Procedures for selection of the optimal network. *Procedia computer science, 123*, 171-176.

Kornas, T., Daub, R., Karamat, M., Thiede, S., & Herrmann, C. (2019). Data-and expert-driven analysis of cause-effect relationships in the production of lithium-ion batteries. *IEEE 15th International Conference on Automation Science and Engineering.* Vancouver.

Kwade, A., Haselrieder, W., Leithoff, R., Modlinger, A., Dietrich, F., & Droeder, K. (2018). Current status and challenges for automotive battery production technologies. *Nature Energy, 3*(4), 290-300.

Li, Y., Liu, K., Foley, A., Zülke, A., Maitane, B., Nanini-Maury, E., Van Mierlo, J., Hoster, H. (2019). Data-driven health estimation and lifetime prediction of lithium-ion batteries: A review. *Renewable and sustainable energy reviews, 113* , 109254.

Lin, J., Liu, X., Li, S., Zhang, C., & Yang, S. (2021). A review on recent progress, challenges and perspective of battery thermal management system. *International Journal of Heat and Mass Transfer, 167*, 120834.

Lipu, M., Hannan, M., Hussain, A., Ayob, A., Saad, M., Karim, T., & How, D. (2020). Data-driven state of charge estimation of lithiumion batteries: Algorithms, implementation factors, limitations and future trends. *Journal of Cleaner Production, 277*, 124110.

Lipu, M., Hannan, M., Karim, T., Hussain, A., Saad, M., Ayob, A., Miah, M.S. Mahlia, T. (2021). Intelligent algorithms and control strategies for battery management system in electric vehicles: Progress, challenges and future outlook. *Journal of Cleaner Production, p.126044, 292*, 126044.

Liu, C., Lin, J., Cao, H., Zhang, Y., & Sun, Z. (2019). Recycling of spent lithium-ion batteries in view of lithium recovery: A critical review. *Journal of Cleaner Production, 228*, 801-813.

Liu, K., Ashwin, T., Xiaosong, H., Lucu, M., & Widanage, D. (2020a). An evaluation study of different modelling techniques for calendar ageing prediction of lithium-ion batteries. *Renewable and Sustainable Energy Reviews, 131*, 110017.

Liu, K., Hu, X., Zhou, H., Tong, L., Widanalage, D., & Marco, J. (2021b). Feature analyses and modelling of lithium-ion batteries manufacturing based on random forest classification. *IEEE/ASME Transactions on Mechatronics, Early Access*.

Liu, K., Wei, Z., Yang, Z., & Li, K. (2021a). Mass load prediction for lithium-ion battery electrode clean production: A machine learning approach. *Journal of Cleaner Production, 289*, 125159.

Liu, Y., Liu, J., Qin, D., Li, G., Chen, Z., & Zhang, Y. (2020b). Online energy management strategy of fuel cell hybrid electric vehicles based on rule learning. *Journal of Cleaner Production, 260*, 121017.

Ma, Y., & Guo, G. (2014). *Support vector machines applications.* New York, NY, USA: Springer.

Mei, W., Chen, H., Sun, J., & Wang, Q. (2019). The effect of electrode design parameters on battery performance and optimization of electrode thickness based on the electrochemical–thermal coupling model. *Sustainable energy & fuels, 3*(1), 148-165.

Mishra, A., Mehta, A., Basu, S., Malode, S., Shetti, N., Shukla, S., Nadagouda, M.N Aminabhavi, T. (2018). Electrode materials for lithium-ion batteries. *Materials Science for Energy Technologies, 1*(2), 182-187.

Mistry, A., Franco, A., Cooper, S., Roberts, S., & Viswanathan, V. (2021). How Machine Learning Will Revolutionize Electrochemical Sciences. *ACS energy letters, 6*(4), 1422-1431.

Myers, R., Montgomery , D., & Anderson-Cook , C. (2016). *Response surface methodology: Process and product optimization using designed experiments.* New Jersey: John Wiley & Sons.

Niri, M., Bui, T., Dinh, T., Hosseinzadeh, E., Yu, T., & Marco, J. (2020a). Remaining energy estimation for lithium-ion batteries via Gaussian mixture and Markov models for future load prediction. *Journal of Energy Storage, 28*, 101271.

Niri, M., Dinh, T., Yu, T., Marco, J., & Bui, T. (2020b). State of Power Prediction for Lithium-Ion Batteries in Electric Vehicles via WaveletMarkov Load Analysis. *IEEE Transactions on Intelligent Transportation Systems*, 1 - 16.

Oehlert, G. (2010). *A first course in design and analysis of experiments.* USA: W. H. Freeman and Company.

Platt, J. (1998). Sequential minimal optimization: A fast algorithm for training support vector machines. *Microsoft Research, Technical Report MSR-TR-98-14*.

Primo, E., Touzin, M., & Franco, A. (2021). Calendering of Li (Ni0. 33Mn0. 33Co0. 33) O2-based cathodes: analyzing the link between process parameters and electrode properties by advanced statistics. *Batteries & Supercaps, 4*(5), 834-844.

Rokach, L., & Maimon, O. (2007). *Data mining with decision trees: theory and applications.* Singapore: World scientific.

Schnell, J., & Reinhart, G. (2016). Quality management for battery production: a quality gate concept. *Procedia CIRP, 57*, 568-573.

Schnell, J., Nentwich, C., Endres, F., Kollenda, A., Distel, F., Knoche, T., & Reinhart, G. (2019). Data mining in lithium-ion battery cell production. *Journal of Power Sources, 413*, 360-366.

Severson, K., Attia,, P., Jin, N., Perkins, N., Yang, Z., Chen, M., Aykol, M., Herring, P.K., Fraggedakis, D. Bazant, M. (2019). Data-driven prediction of battery cycle life before capacity degradation. *Nature Energy, 4*(5), 383-391.

Shawe-Taylor, J., & Cristianini, N. (2004). *Kernel Methods for Pattern Analysis.* New York: Cambridge University Press.

Steinberg, D. (1996). Robust design: Experiments for improving quality. *7 Robust design: Experiments for improving quality, 13*, 199240.

Suthaharan, S. (2016). Decision tree learning. In *In Machine Learning Models and Algorithms for Big Data Classification* (pp. 237-269). New York, USA: Springer.

Tange, R., Rasmussen, M., Taira, E., & Bro, R. (2017). Benchmarking support vector regression against partial least squares regression and artificial neural network: Effect of sample size on model performance. *Journal of Near Infrared Spectroscopy, 25*(6), 381-390.

Thiede, S., Turetskyy, A., Kwade, A., Kara, S., & Herrmann, C. (2019). Data mining in battery production chains towards multi-criterial quality prediction. *CIRP Annals - Manufacturing Technology, 68*, 463-466.

Thomitzek, M., Schmidt, O., Röder, F., Krewer, U., Herrmann, C., & Thiede, S. (2018). Simulating process-product interdependencies in battery production systems. *Procedia CIRP, 72*, 346-351.

Tian, J., Wang, Y., & Chen, Z. (2021). An improved single particle model for lithium-ion batteries based on main stress factor compensation. *Journal of Cleaner Production, 278, p.123456., 278*, 123456.

Tropsha, A., Gramatica, P., & Gombar, V. (2003). The importance of being earnest: validation is the absolute essential for successful application and interpretation of QSPR models. *QSAR & Combinatorial Science, 22*(1), 69-77.

Turetskyy, A., Thiede, S., Thomitzek, M., von Drachenfels, N., Pape, T., & Herrmann, C. (2020). Toward data-driven applications in lithium-ion battery cell manufacturing. *Energy Technology, 8*(2), 1900136.

Turetskyy, A., Wessel, J., Herrmann, C., & Thiede, S. (2021). Battery production design using multi-output machine learning models. *Energy Storage Materials, 38*, 93-112.

Väyrynen, A., & Salminen, J. (2012). Lithium ion battery production. *The Journal of Chemical Thermodynamics, 46* , 80-85.

Wu, J., Wei, Z., Liu, K., Quan, Z., & Li, Y. (2020). attery-involved Energy Management for Hybrid Electric Bus Based on Expert-assistance Deep Deterministic Policy Gradient Algorithm. *IEEE Transactions on Vehicular Technology, 69*(11), 12786-12796.

Xu, H., Caramanis, C., & Mannor, S. (2014). A robust leasts quares support vector machine for regression and classification with noise. *Neurocomputing, 140*, 41–52.

Zwicker, M., Moghadam, M., Zhang, W., & Nielsen, C. (2020). Automotive battery pack manufacturing–a review of battery to tab joining. *Journal of Advanced Joining Processes, 1*, 100017.